



Research paper

Identification of furo[2,3-*d*]pyrimidin-4-ylsulfanyl-1,3,4-thiadiazole derivatives as novel FLT3-ITD inhibitors

Mahfam Moradi^{a,b,1}, Alireza Mousavi^{a,b,1}, Eva Řezníčková^{c,1}, Fariba Peytam^d, Miroslav Peřina^c, Veronika Vojáčková^c, Loghman Firoozpour^b, Radek Jorda^c, Jiří Grúz^c, Zahra Emamgholipour^b, Seyed Esmaeil Sadat-Ebrahimi^b, Vladimír Kryštof^{c,e,*}, Alireza Foroumadi^{b,d,**}

^a International Campus-School of Pharmacy, Tehran University of Medical Sciences, Tehran, Iran

^b Department of Medicinal Chemistry, Faculty of Pharmacy, Tehran University of Medical Sciences, Tehran, Iran

^c Department of Experimental Biology, Faculty of Science, Palacký University Olomouc, Šlechtitelů 27, 78371, Olomouc, Czech Republic

^d Drug Design and Development Research Center, The Institute of Pharmaceutical Sciences, Tehran University of Medical Sciences, Tehran, Iran

^e Institute of Molecular and Translational Medicine, Faculty of Medicine and Dentistry, Palacký University, Olomouc, Czech Republic

ARTICLE INFO

Keywords:

AML
FLT3-ITD inhibitors
furo[2,3-*d*]pyrimidine
1,3,4-thiadiazole
urea

ABSTRACT

Given the significant prevalence of FLT3 receptor and its mutations in acute myeloid leukemia (AML) pathogenesis, we present a novel series of furo[2,3-*d*]pyrimidin-1,3,4-thiadiazole-urea derivatives, designed to exhibit FLT3-ITD inhibitory activity. These compounds demonstrated cytotoxicity in FLT3-ITD expressing AML cell lines MOLM-13 and MV4-11 in the nanomolar range, with significant selectivity over the K562 cell line. In-depth evaluations of example compound **49** revealed its efficacy in suppressing FLT3 phosphorylation and the downstream signaling molecules, including STAT5 and ERK1/2. Notably, compound **49** demonstrated cytotoxic effects in Ba/F3 cells expressing FLT3-ITD or FLT3-ITD-F691L mutant, exceeding the potency of both sorafenib and quizartinib. Molecular docking studies suggest that this compound binds to the active site of FLT3 in a type II manner. The study suggests that substituted furo[2,3-*d*]pyrimidines could be useful additions to the growing field of FLT3-targeted therapy for AML. These compounds have the potential to serve as novel FLT3-ITD inhibitors and may offer insights for developing future therapeutic strategies in AML.

1. Introduction

Acute myeloid leukemia (AML) is a highly aggressive and heterogeneous hematologic malignancy characterized by the rapid proliferation of immature myeloid cells in the bone marrow and blood [1]. Currently, the number of adult patients diagnosed with AML exceeds a quarter of a million annually. Despite significant advances in the treatment of AML over the past few decades, two-thirds of young adults and 90% of older adults still succumb to the disease [2]. The high mortality rate highlights the urgent need for further research and novel therapeutic candidates to improve the survival rates and overall outcome for AML patients [3]. Among the diverse molecular alterations driving AML pathogenesis, mutations in the FMS-like tyrosine kinase 3 (FLT3) gene

have emerged as a prevalent and clinically significant target [4].

As a type III receptor tyrosine kinase family member, FLT3 plays a significant role in maintaining the immune response, hematopoiesis, and cellular proliferation. FLT3 consists of an extracellular ligand-binding domain (ECD), a transmembrane domain (TMD), a juxtamembrane domain (JMD), and cytoplasmic tyrosine kinase domain (TKD) [5]. Upon binding to its cognate ligand (FL), FLT3 undergoes autophosphorylation, activating downstream signaling cascades crucial for cellular growth and survival [6]. The major intracellular signaling pathways triggered by FLT3 include the Ras/Raf/MEK/ERK pathway, which primarily governs cell proliferation, and the PI3K/Akt/mTOR pathway, involved in cell survival and anti-apoptotic responses [7].

Two types of mutations are regularly observed in the FLT3 receptor.

* Corresponding author. Department of Experimental Biology, Faculty of Science, Palacký University Olomouc, Šlechtitelů 27, 78371, Olomouc, Czech Republic.

** Corresponding author. Department of Medicinal Chemistry, Faculty of Pharmacy, Tehran University of Medical Sciences, Tehran, Iran.

E-mail addresses: vladimir.krystof@upol.cz (V. Kryštof), aforoumadi@yahoo.com (A. Foroumadi).

¹ These authors contributed equally to this work.

FLT3-ITD (Internal Tandem Duplication) mutation can be found in approximately 25–30% of AML patients and is associated with poor prognosis and increased resistance to conventional therapies. This mutation is characterized by the insertion of tandem duplications of internal sequences within the juxtamembrane domain of the FLT3 receptor tyrosine kinase [8,9]. Consequently, the mutant FLT3 receptor gains constitutive and ligand-independent activation, triggering downstream signaling cascades involved in cell proliferation, survival, and resistance to apoptosis of hematopoietic progenitor cells. FLT3-TKD mutations are another significant molecular alterations found in approximately 5% of AML cases [10] and typically involve substitutions at the D835 residue within the activation loop [11].

First-generation FLT3 inhibitors, such as sorafenib [12], sunitinib [13], tandutinib [14], midostaurin (2016 FDA-approved) [15], and lestaurtinib [16], were initially developed based on their activity against other kinases, and their potential as FLT3 inhibitors was subsequently explored. While these compounds showed promising inhibitory activity against FLT3-ITD, they also displayed limited selectivity, leading to off-target effects and potential toxicities. Additionally, resistance to first-generation FLT3 inhibitors has emerged as a significant challenge, partially due to mutations within the FLT3 kinase domain [17]. To address these limitations, second-generation FLT3 inhibitors were developed, including gilteritinib (2019 FDA-approved) [18], crenolanib [19], tuspentinib [20], and quizartinib [21] (recently approved by the FDA in July 2023 for newly diagnosed FLT3-ITD positive adult AML patients, utilizing standard induction, consolidation, or maintenance monotherapy with cytarabine and anthracycline regimens for FLT3-ITD positive AML). These compounds demonstrated improved selectivity and potency against FLT3-ITD and FLT3-TKD mutants. Additionally, they have shown enhanced tolerability and manageable toxicities, making them well-suited for combination therapies. Despite these advancements, the duration of response is still unsatisfactory due to the resistance mechanisms to second-generation FLT3 inhibitors. Therefore, there is a need to overcome drug resistance and optimize treatment for FLT3-driven AML [22]. Considering the remarkable role of FLT3 in regulatory cellular processes, the discovery and development of inhibitors of this kinase has become a promising approach in current studies [23].

There are three types of FLT3 inhibitors based on their binding mode: firstly, type I inhibitors (also known as ATP-competitive inhibitors) occupy the ATP-binding pocket of the FLT3 receptor in the active DFG-in conformation [24]. Secondly, type II inhibitors target an allosteric site adjacent to the ATP-binding pocket created by DFG motif shifting [25]. Thirdly, type I/II inhibitors have emerged as a more recently developed class of inhibitors having substantial characteristics of both type I and type II inhibitors, as they can bind to both the ATP-binding pocket (type I-like) and an additional allosteric site (type II-like) [26,27].

According to the literature, type II inhibitors interact with three critical segments in the FLT3 receptor structure: (1) the hinge binder making crucial interactions with C694 and E692 motifs, (2) the DFG interactor moiety binding to F691 residue, (3) the terminal lipophilic site interacting with the allosteric area created by DFG shifting (Fig. 1) [28].

In recent years, the furanopyrimidine core has been reported several times as a promising scaffold for designing kinase inhibitors as a hinge-binding motif targeting different enzymes like Aurora [29], EGFR [30], c-Met [31], VEGFR-2 [32], and FLT3 [33]. Although these compounds showed potential for kinase inhibition, none was both selective and potent against FLT3 kinase. However, introducing a 1,3,4-thiadiazole-urea moiety at the C-4 position of the quinazoline ring led to the discovery of a selective and potent FLT3 inhibitor [34]. Building upon this finding, our research group reported several cytotoxic agents by linking this moiety as a possible DFG-binding motif to various heterocyclic rings [35,36].

In an effort to present novel and potential FLT3 inhibitors, we describe here the rational design, synthesis and biological evaluation of furo[2,3-*d*]pyrimidin-1,3,4-thiadiazole derivatives.

2. Results and discussion

2.1. Design and synthesis

Continuing with our previous studies, herein, by drawing inspiration from the structural diversity offered by the furo[2,3-*d*]pyrimidine core and the 1,3,4-thiadiazole-urea moiety, we pursued a rational hybridization strategy intending to develop new candidates against AML, able to target FLT3 kinase and its mutants (Fig. 2).

The targeted furo[2,3-*d*]pyrimidines were obtained through two multi-step synthetic approaches, as outlined in Schemes 1 and 2. 1,3,4-Thiadiazole-urea derivatives 3–16 were obtained through the reaction between thiosemicarbazide 1 and carbon disulfide to afford 5-amino-1,3,4-thiadiazole-2-thiol 2, followed by reaction with substituted phenyl isocyanates (to give compounds 3–16) [35,37]. In another procedure, adduct 2 underwent the amidation reaction with benzoyl chloride intermediate, obtained from the condensation of benzoic acid and thionyl chloride (to give compound 17) [38,39].

The synthetic methods to afford furo[2,3-*d*]pyrimidine skeletons, considering their substituents at C-5 and/or C-6 positions, were initiated through the condensation of malononitrile with two different compounds. The synthesis protocol involved starting the 5,6-diphenylfuranopyrimidine analog with benzoin, and the 6-arylfuranopyrimidine analog with substituted phenacylbromides. Subsequent steps, including cyclization using formic acid and acetic anhydride, as well as chlorination using POCl₃, were common for both series.

Finally, nucleophilic aromatic substitution between chlorine moiety of compounds 21, 44, and 45 with various substituted 1,3,4-thiadiazoles 3–17 was performed to synthesize desirable substituted furo[2,3-*d*]pyrimidines 22–36 and 46–61. The structures of the isolated compounds were deduced based on their IR, ¹H, and ¹³C NMR spectroscopy, high-resolution mass spectrometry, and elemental analysis. Furthermore, the purity was confirmed using HPLC. Partial assignments of these resonances are given in the Experimental Part.

2.2. FLT3-ITD inhibitory activity and antiproliferative assays

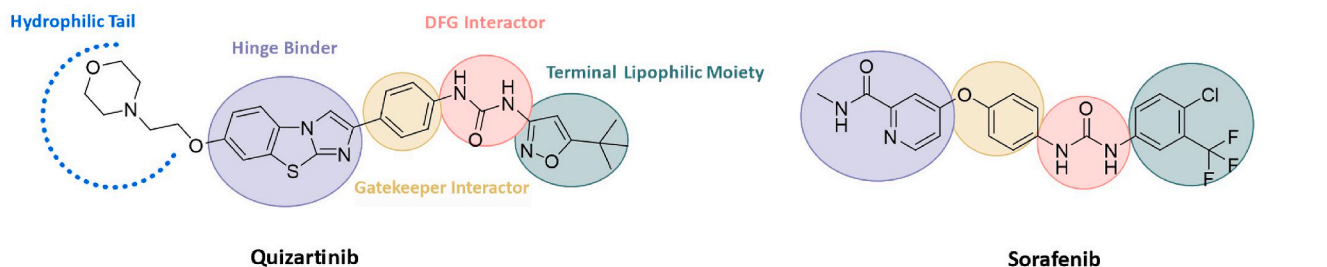


Fig. 1. Quizartinib and sorafenib representing type II inhibitors.

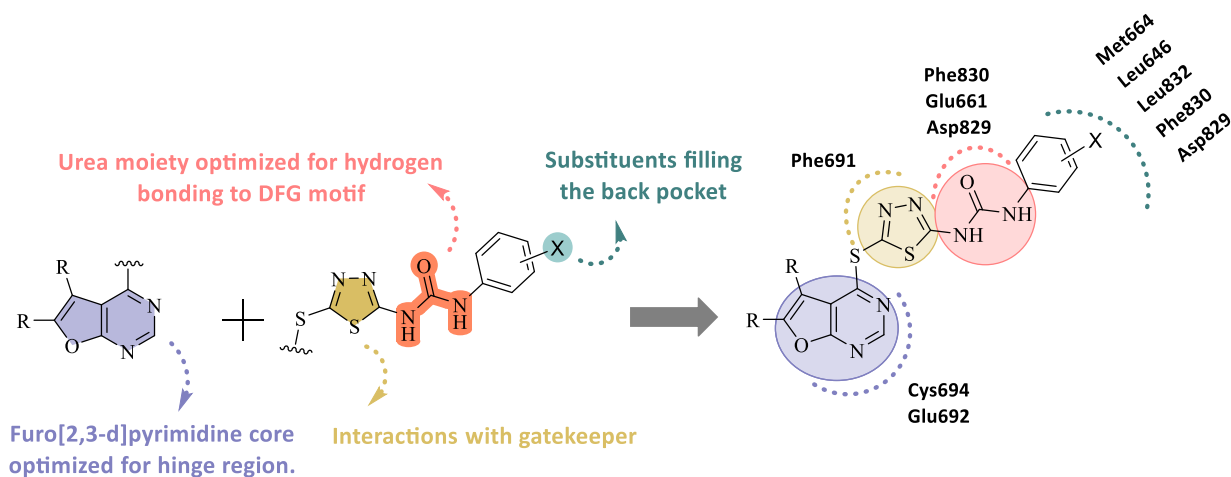
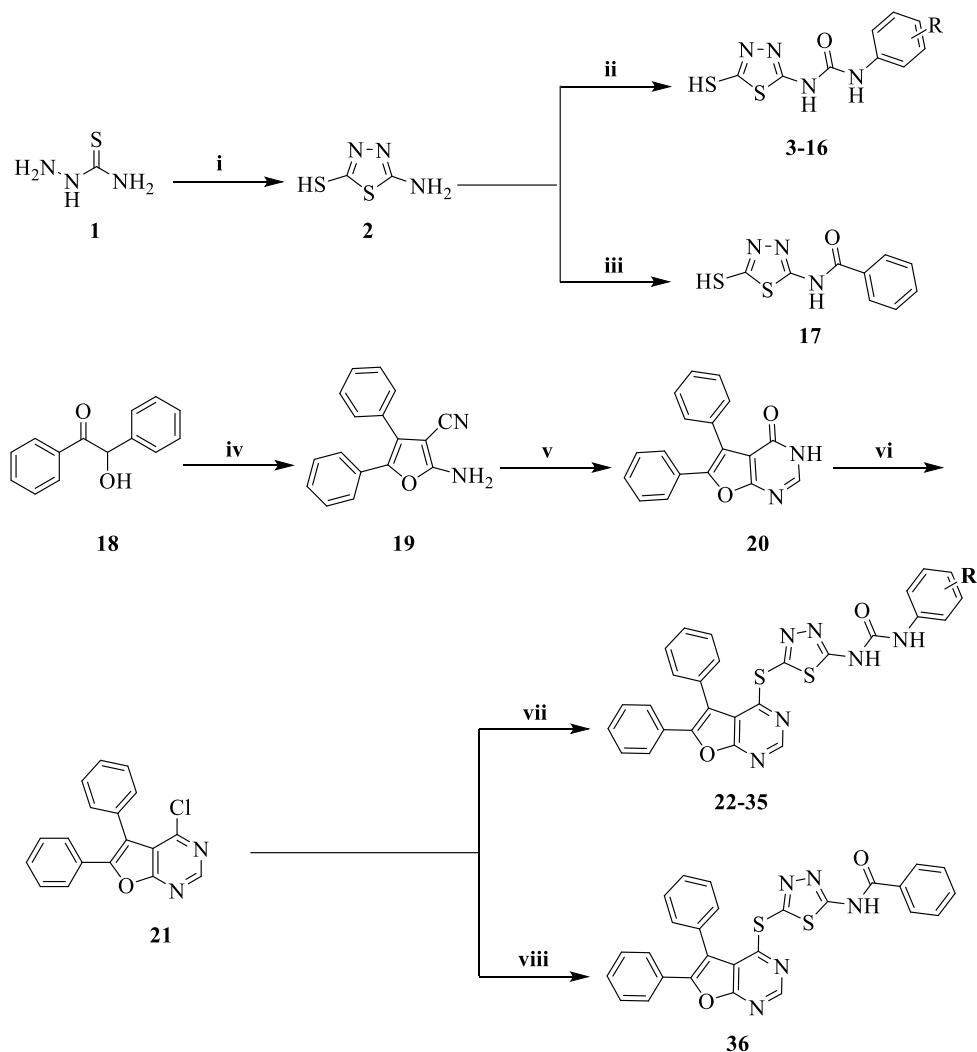
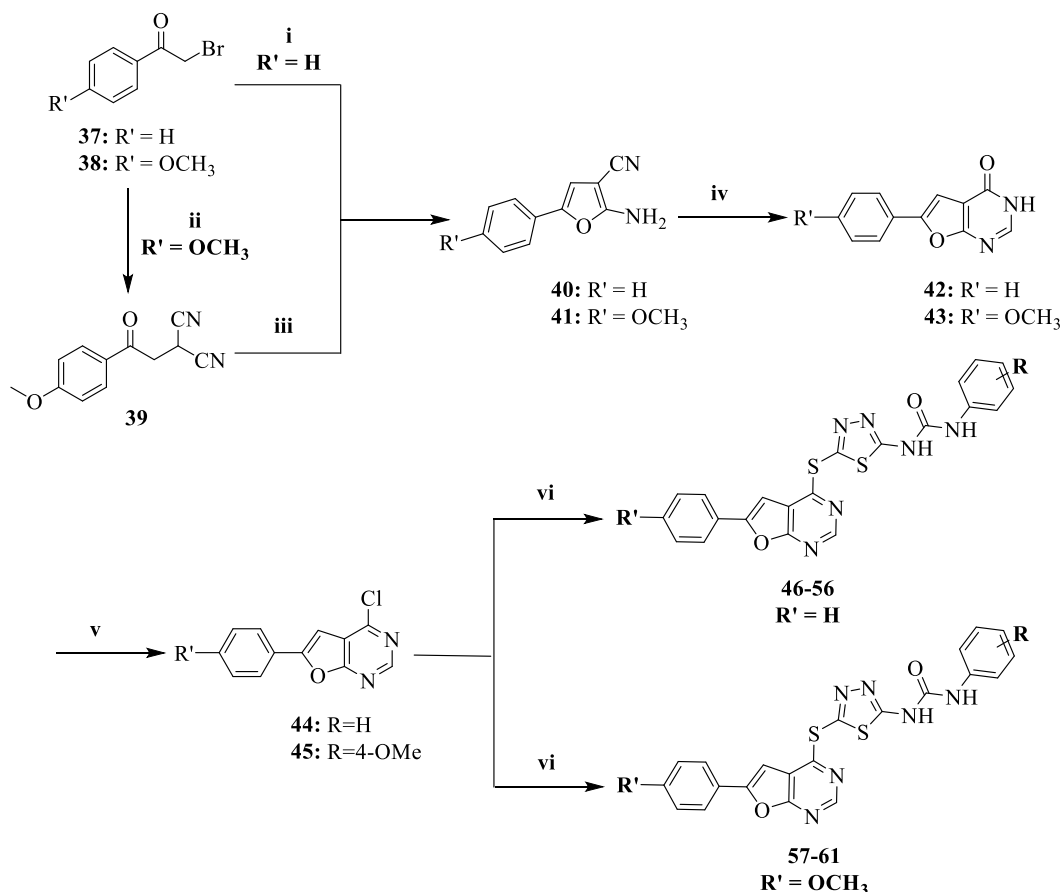


Fig. 2. Design of targeted furo[2,3-d]pyrimidines bearing 1,3,4-thiadiazole-urea moiety.



Scheme 1. Reagents and conditions for the synthesis of 5,6-diphenylfuranopyrimidine analogs 22–36: i) CS_2 , Na_2CO_3 , dry EtOH, reflux, 8 h; ii) Various substituted phenyl isocyanates, dry DCM, r.t., 24 h; iii) benzoic acid in SOCl_2 , reflux, 2 h; then compound 2, Et_3N , dry DMF, r.t., 12 h; iv) malononitrile, Et_2NH , DMF, r.t., 24h; v) formic acid, acetic anhydride, reflux, 16 h; vi) POCl_3 , 100 °C, 2 h; vii) Et_3N , EtOH, reflux, 24h; viii) Et_3N , CH_3CN , reflux, 24 h.



Scheme 2. Reagents and conditions for the synthesis of 6-arylfuranopyrimidine analogs **46–61**: i) Et₂NH, DMF, r.t., 16h; ii) NaOH, EtOH, 0 °C, 30 min; iii) Et₂NH, DMF, r.t., 12 h; iv) formic acid, acetic anhydride, reflux, 24 h; v) POCl₃, 100 °C, 2 h; vi) Et₃N, EtOH, reflux, 24 h.

derivatives **22–35** and **46–61** bearing one or two phenyl rings at C-5 and/or C-6 positions of furopyrimidine backbone, as well as different substituents on the terminal phenyl rings were evaluated for their inhibitory activities against FLT3-ITD accompanied with anti-proliferative activities of compounds against K562 (FLT3 independent), MV4-11 (homozygous FLT3-ITD), and MOLM-13 (heterozygous FLT3 wt/ITD) cell lines. The results are summarized in Table 1.

Overall, 27 out of 31 compounds demonstrated outstanding FLT3-ITD inhibition at the nanomolar levels, with 12 compounds exhibiting single-digit IC₅₀ values. Furthermore, 22 and 23 compounds showed IC₅₀ values below 1 μM against MV4-11 and MOLM-13 cell lines, respectively. Additionally, almost all compounds showed excellent selectivity against FLT3-ITD-positive cell lines over the FLT3-independent K562 cell line. To describe the correlations between structures and observed activities, compounds were divided into three categories according to the substituents on the furo[2,3-*d*]pyrimidine backbone: (1) compounds **22–35** containing 5,6-diphenyl substituents; (2) compounds **46–56** containing unsubstituted phenyl ring at C-6 position; (3) compounds **57–61** containing 4-methoxy substituted phenyl ring at C-6 position.

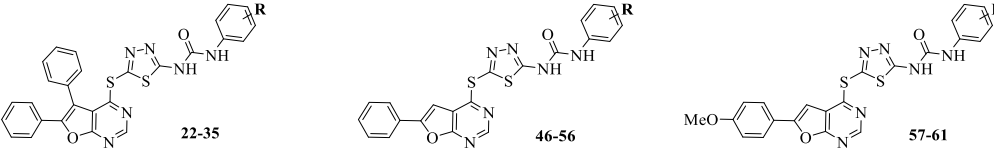
In the first series, compound **22**, with an unsubstituted terminal phenyl, exhibited notable FLT3-ITD inhibitory potency (IC₅₀ = 0.004 μM) and great anti-proliferative activity (GI₅₀s 0.074 μM and 0.110 μM against MV4-11 and MOLM-13, respectively). Introducing a substituent, whether electron-donating group (EDG) or electron-withdrawing group (EWG), at different positions of the phenyl ring (compounds **23–31**) did not improve the activity compared to compound **22** (IC₅₀ values ranging from 0.004 μM to 0.055 μM). Regarding their anti-proliferative activities, almost all compounds exhibited better activity against MV4-11 than MOLM-13. The presence of halogen caused a detrimental effect,

while the presence of EDGs (like methoxy or methyl) led to an improvement in potency. For example, compound **26**, bearing 4-OCH₃, exhibited even better activity (GI₅₀ = 0.061 μM and 0.083 μM against MV4-11 and MOLM-13, respectively) than compound **22**. Introducing a second substituent at the different positions of terminal phenyl (compounds **32–35**) caused a decrease in both enzymatic and cellular potency. Among them, compound **33**, with 2,4-diF substituents, displayed better activities with an IC₅₀ value of 0.006 μM against FLT3-ITD, as well as GI₅₀ values of 0.169 μM and 0.164 μM against MV4-11 and MOLM-13, respectively.

In the second series, compound **46**, bearing unsubstituted terminal phenyl, showed an IC₅₀ value of 0.038 μM against FLT3-ITD and GI₅₀ values of 0.165 μM and 0.087 μM against MV4-11 and MOLM-13, respectively. Interestingly, there were three contradictions between this series and the first series: (1) the presence of any substituents (whether EDG or EWG, except 3-F) on the phenyl ring (compounds **47–56**) led to an increase in the potency. (2) Compound **53** (bearing 4-Br) and compounds **54** and **56** (bearing di-substituents) exhibited the most potent inhibitory activity with an IC₅₀ value of 0.003 μM (3) Nearly all compounds demonstrated better antiproliferative activity against MOLM-13 than MV4-11. Introducing 4-OCH₃ at the phenyl ring (compound **49**) improved cellular activity and induced considerable cell cycle arrest at G1 phase, surpassing all other compounds and making this compound an appropriate choice for further investigations.

In the third series, a methoxy group was introduced at the para position of the phenyl ring, which was substituted on the C-6 position of the furopyrimidine backbone. This particular moiety was selected because it could potentially be replaced with traditional hydrophilic substituents in further studies to improve pharmacokinetic properties. In this series, compound **57**, having unsubstituted terminal phenyl ring,

Table 1
FLT3-ITD-inhibitory and cellular activities of furo[2,3-*d*]pyrimidine-1,3,4-thiadiazole-aryl urea derivatives **22–35** and **46–61**.



Cmpd.	R	IC ₅₀ ± SD (μM) ^a				Cell cycle ^b % G1 phase
		FLT3-ITD	K562	MV4-11	MOLM-13	
22	H	0.004 ± 0.001	>10	0.074 ± 0.026	0.110 ± 0.024	89.9
23	3-CH ₃	0.010 ± 0.003	>10	0.115 ± 0.021	0.120 ± 0.014	84.0
24	4-CH ₃	0.005 ± 0.002	>10	0.134 ± 0.066	0.194 ± 0.025	71.4
25	3-OCH ₃	0.004 ± 0.001	9.950 ± 0.071	0.086 ± 0.044	0.185 ± 0.033	73.8
26	4-OCH ₃	0.005 ± 0.002	>10	0.061 ± 0.012	0.083 ± 0.004	74.8
27	3-F	0.004 ± 0.000	>10	0.145 ± 0.021	0.650 ± 0.127	69.1
28	3-Cl	0.014 ± 0.007	>10	0.362 ± 0.004	0.404 ± 0.019	71.8
29	4-Cl	0.016 ± 0.006	9.865 ± 0.191	0.342 ± 0.045	0.452 ± 0.086	66.4
30	2-Br	0.004 ± 0.004	>10	0.290 ± 0.057	0.427 ± 0.115	70.1
31	4-Br	0.055 ± 0.007	>10	0.396 ± 0.114	0.723 ± 0.146	64.0
32	3-Cl-4-CH ₃	>5	>10	>10	>10	63.8
33	2,4-diF	0.006 ± 0.002	>10	0.169 ± 0.012	0.164 ± 0.020	76.2
34	3,4-diCl	0.455 ± 0.183	>10	6.190 ± 0.269	8.655 ± 1.902	61.0
35	4-Cl-3-CF ₃	1.269 ± 0.574	>10	8.304 ± 1.649	>10	61.0
46	H	0.038 ± 0.025	>10	0.165 ± 0.007	0.087 ± 0.010	91.4
47	3-CH ₃	0.012 ± 0.001	>10	0.133 ± 0.052	0.105 ± 0.007	91.4
48	3-OCH ₃	0.017 ± 0.005	9.455 ± 1.080	0.120 ± 0.014	0.079 ± 0.002	94.7
49	4-OCH ₃	0.031 ± 0.009	>10	0.105 ± 0.007	0.063 ± 0.004	94.9
50	3-F	0.056 ± 0.026	7.960 ± 1.188	0.337 ± 0.117	0.190 ± 0.000	83.3
51	3-Cl	0.010 ± 0.004	>10	0.345 ± 0.021	0.240 ± 0.085	89.0
52	4-Cl	0.009 ± 0.006	>10	0.430 ± 0.127	0.297 ± 0.168	89.2
53	4-Br	0.003 ± 0.001	>10	1.190 ± 1.047	0.570 ± 0.251	67.7
54	3-Cl-4-CH ₃	0.003 ± 0.000	9.495 ± 1.010	0.430 ± 0.085	0.375 ± 0.064	81.2
55	3,4-diCl	0.004 ± 0.000	9.830 ± 0.240	1.030 ± 0.438	0.710 ± 0.240	64.0
56	4-Cl-3-CF ₃	0.003 ± 0.000	>10	0.910 ± 0.113	1.220 ± 0.321	73.6
57	H	0.016 ± 0.001	>10	0.096 ± 0.013	0.117 ± 0.055	91.6
58	4-OCH ₃	0.023 ± 0.003	>10	0.250 ± 0.014	0.180 ± 0.014	85.4
59	3-Cl	0.048 ± 0.035	>10	1.555 ± 0.629	1.065 ± 0.035	67.7
60	4-Cl	0.022 ± 0.015	>10	1.385 ± 0.035	1.140 ± 0.071	65.3
61	4-Cl-3-CF ₃	0.055 ± 0.027	>10	>10	5.815 ± 0.813	63.6
SORA		0.037 ± 0.003	>10	0.005 ± 0.004	0.038 ± 0.003	93.8
QUIZ		0.030 ± 0.006	>10	0.003 ± 0.003	0.003 ± 0.003	94.3

^a measured at least in duplicate.

^b proportion of the MV4-11 cells in the G1 phase of the cycle after the treatment with 80 nM concentration of the representative compound for 24 h. Percentage of the cells in the G1 phase of the cell cycle in untreated samples was 62.5 ± 1.1 %. SORA, sorafenib and QUIZ, quizartinib were used as standards.

displayed the most favorable enzymatic and cellular potencies with IC₅₀ value of 0.016 μM against FLT3-ITD and GI₅₀ 0.096 μM and 0.117 μM against MV4-11 and MOLM-13, respectively. Introducing one or two substituents (whether EDG or EWG) at different positions of this phenyl caused detrimental effects on the activities, particularly in cellular assessments.

To highlight the role of the urea functionality on the FLT3 inhibitory activity of these compounds, this moiety was replaced with an amide, resulting in compound **36** (Scheme 1), which exhibited complete inactivity in both cellular (GI₅₀ > 10 μM in K562, MV4-11 and MOLM-13 cells) and enzymatic (IC₅₀ > 5 μM) assays.

In conclusion, most of the compounds exhibited great to outstanding inhibitory potencies, whether in enzymatic or in cellular assessments. Drug-like properties and preliminary ADME predictions were assessed using the online tool SwissADME, which predicted lower water solubility for some of the compounds, though it was comparable to that of reference drugs such as sorafenib and quizartinib (see Supplementary data). Importantly, water solubility was not an issue in practice. Additionally, reasonable metabolic stability of compound **49** was determined using isolated human liver microsomes (Fig. S1). To obtain more information about the inhibition mechanism of substituted furo[2,3-*d*]pyrimidine-1,3,4-thiadiazole-aryl ureas, compound **49**, considering its noticeable potency with 95% G1 phase arrest in MV4-11 cells, was selected for further evaluations.

2.3. Molecular docking studies

Molecular modelling studies were conducted to characterize the binding mode of compound **49** in FLT3 binding site. Considering the structural similarity of our candidate with quizartinib and also its FLT3 kinase inhibitory activities in ITD and TKD mutants, the kinase co-crystal with quizartinib (PDB: 4XUF) [40] was selected as a molecular docking target. In the crystal structure, the DFG motif adopts a “DFG-out” orientation, with F830 pointing into the active site.

The best docking pose of compound **49** was located in the binding site between the N lobe and the C lobes, analogous to quizartinib, with corresponding conserved interactions. The position of the inhibitor in the inactive kinase conformation suggested that it was a type II inhibitor. The methoxyphenyl moiety of compound **49** was deeply buried in the hydrophobic pocket formed by M664 and M665 from the αC helix, I674 in the N lobe and L802 with H809, directly adjacent to the DFG motif (Fig. 3). Analogous position and interactions have been described for the *tert*-butyl substituent on the isoxazole ring of quizartinib. Hydrophobic pocket-binding is also known to increase the selectivity of FLT3 inhibitors.

The urea motif of the candidate compound established a typical hydrogen bond network: its carbonyl group engaged in a hydrogen bond with the backbone nitrogen of D829, while its secondary amines formed two hydrogen bond interactions with E661. The central thiadiazole ring

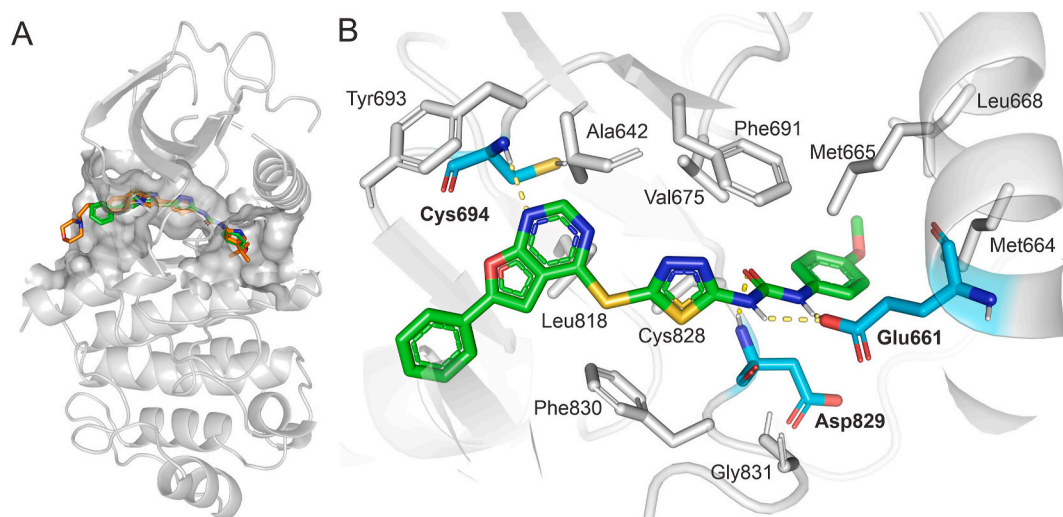


Fig. 3. Binding pose of compound **49** in the crystal structure of FLT3 (PDB: 4XUF). **A**, **49** (green sticks) and quizartinib (orange sticks) with shown surface of the binding site. **B**, detailed view on the interactions; side chains of interacting residues with hydrophobic or π interaction are shown as grey sticks. Amino acid residues forming the hydrogen bonds are shown with main and side chains as cyan sticks. Other atoms are coloured as follows: nitrogens (blue), oxygens (red), sulphur (yellow) and polar hydrogens (white).

was positioned by π - π interactions with the gatekeeper F691 and the F830 from the DFG motif, analogous to central imidazobenzothiazole in quizartinib. The nitrogen atom N1 in the furo[2,3-*d*]pyrimidine ring formed a typical hydrogen bond with the backbone nitrogen of C694, accompanied by hydrophobic interactions with A642 and L818. The C-6 substituted phenyl moiety was located at the entrance to the binding site in the hinge region and also made an interaction with L616 (Fig. 3). Moreover, the binding energies, evaluated in AutoDock Vina software, were -10.7 kcal/mol and -11.5 kcal/mol for compound **49** and quizartinib, respectively.

The interactions of selected compounds from the three categories were examined to confirm the SAR from the target's structure perspective. In contrast to category 2 (represented by compound **49** with an unsubstituted phenyl ring at the C-6 position), compounds **22–35** from category 1 bound to the active cavity more shallowly (with smaller binding energies), with the 5,6-diphenyl motif located at the entrance and pointing out. While compound **22** with an unsubstituted terminal phenyl showed conservative binding, bulky substituents and combinations of 3- and 4-substitutions in compounds **32**, **34**, and **35** could hinder tight binding and inhibitory properties, corresponding with the impaired activity.

Despite the extensive binding network and deeper position of **49**, FLT3-inhibitory activity was not enhanced compared to compound **22** across category 2 (compounds **46–56**). However, compounds with 3- and 4-substitutions (**54–56**) displayed the terminal phenyl position in the wider part of the cavity, allowing substitutions without surface collisions leading to retained enzyme inhibitory activity. The presence of a 4-methoxy substituted phenyl ring at the C-6 position (compounds **57–61**) did not affect the binding mode, as the C-6 phenyl ring points out of the binding cavity.

The key compound underlining the pivotal role of urea motif is **36**, where the replacement with an amide lead to the absence of hydrogen bond with E661 and possible change in terminal phenyl orientation, leading to inactivity in both cellular and enzymatic assays.

2.4. Selectivity and mechanistic study

To confirm the promising FLT3-ITD inhibitory activity of compound **49** in a cellular context, we performed the NanoBRET target engagement assay in HEK293 cells (Fig. 4). The effect of **49** was compared to sorafenib used as a standard. The results confirmed inhibition of FLT3 in

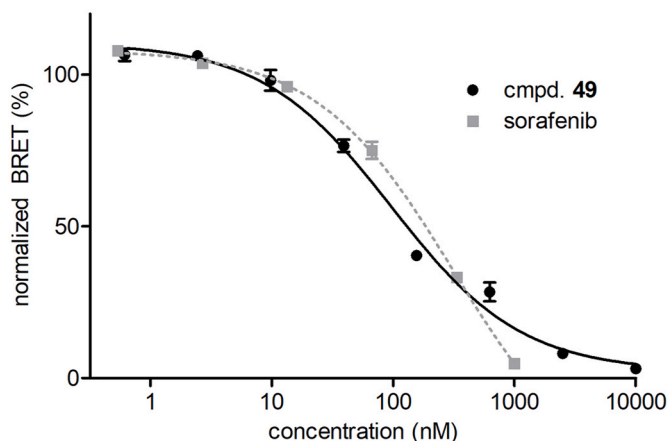


Fig. 4. Cellular FLT3 engagement using NanoBRET technology.

cells with similar activities obtained for both compounds tested (IC_{50} values of 174 nM and 183 nM for **49** and sorafenib, respectively).

To determine whether the example compound **49** had the required selectivity in addition to its promising FLT3-ITD inhibitory activity, **49** was evaluated in a panel of 50 additional kinases across the human kinome (Fig. 5). The results showed that at a concentration of 1 μ M, compound **49** did not significantly affect any of the kinases tested, with the exception of TrkA where residual kinase activity dropped slightly below 50%.

All of the abovementioned results confirmed the suitability of compound **49** as the lead compound of the series for further biological profiling. Compound **49** showed promising biological activities, such as a low nanomolar IC_{50} value against recombinant FLT3-ITD (0.031 μ M) and a beneficial selectivity ratio between FLT3-dependent (MV4-11 and MOLM-13) and FLT3-independent (K562) cells.

While the proliferation of K562 was not significantly affected by the concentration up to 10 μ M, the GI_{50} values obtained for MV4-11 and MOLM-13 were a hundred times lower (0.105 μ M for MV4-11 and 0.063 μ M for MOLM-13). In addition, cell cycle analysis of MV4-11 cells treated with compound **49** showed that a concentration as low as 3.2 nM increased the number of cells in the G1 phase of the cell cycle in comparison to untreated control cells. Higher concentrations induced more

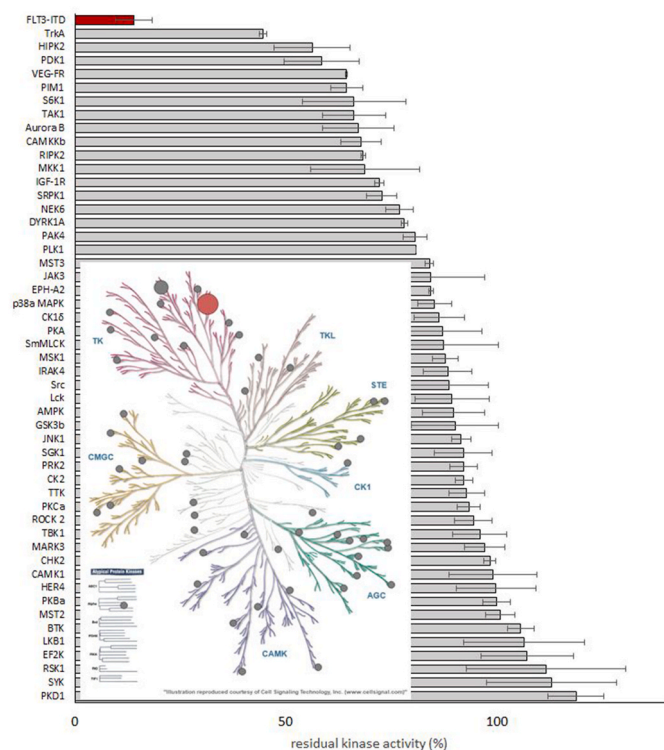


Fig. 5. Kinase selectivity profiling of 49 at a concentration of 1 μM against selected human kinases. Inset shows the kinome coverage.

than 90% G1 phase cell cycle arrest, accompanied by a concentration-dependent increase in cells in the subG1 phase, corresponding to the cells undergoing cell death. On the other hand, the FLT3-independent cell line HL60 was not affected in the same concentration range of 49 and no changes in cell cycle phase distribution or dose-dependent increases in subG1 populations were observed (Fig. 6). This result was consistent with the evaluation of the antiproliferative properties of 49 in this cell line, showing that these cells were not affected by compound 49 up to 10 μM after 72 h (Table 2).

The link between the G1 phase cell cycle arrest induced by compound 49 in MV4-11 and the inhibition of FLT3 signaling was further confirmed by immunoblotting analysis of MV4-11 cells treated with increasing concentrations of 49 for 1 h. The dose-dependent attenuation of FLT3 autophosphorylation (Y589/591), as well as reduced phosphorylation of FLT3 downstream targets (Y694 of STAT5 and T202/Y204 of ERK1/2), clearly demonstrated the FLT3-dependent mechanism

Table 2
Antiproliferative activities of compound 49, sorafenib, and quizartinib.

cell line	GI ₅₀ (μM) ± SD ^a		
	Compound 49	sorafenib	quizartinib
HL60	>10	2.813 ± 0.750	>10
Kasumi-1	3.057 ± 1.011	0.079 ± 0.017	0.016 ± 0.004
EOL-1	0.039 ± 0.020	<0.003	<0.003
Ba/F3 parental	>10	8.915 ± 0.151	3.029 ± 0.367
Ba/F3-FLT3-ITD	0.054 ± 0.004	0.004 ± 0.001	0.003 ± 0.000
Ba/F3-FLT3-ITD-F691L	0.277 ± 0.034	2.611 ± 0.663	0.502 ± 0.115

^a measured at least in duplicate.

of action of compound 49 (Fig. 7).

The use of FLT3 inhibitors is often limited by the negative biological properties of the molecules. One of these limitations is the potent inhibition of unsuitable off-targets, another is the onset of mutations in the FLT3 gene caused by the inhibitor, leading to resistance to the treatment [41,42]. Therefore, we expanded the panel of evaluated cell lines for candidate compound 49 and compared its efficacy with sorafenib and

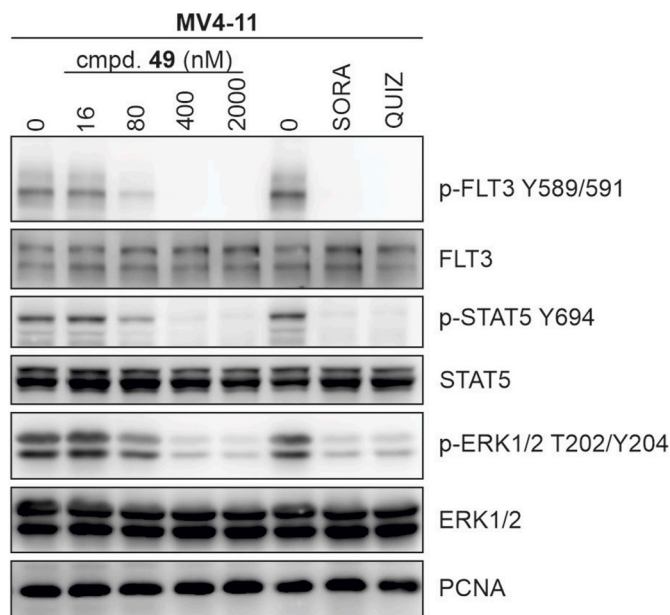


Fig. 7. Immunoblotting analysis of the phosphorylation status of FLT3 and its downstream targets in MV4-11 cells treated with 49 for 1 h. Sorafenib (SORA; 50 nM) and quizartinib (QUIZ; 50 nM) were used as standards.

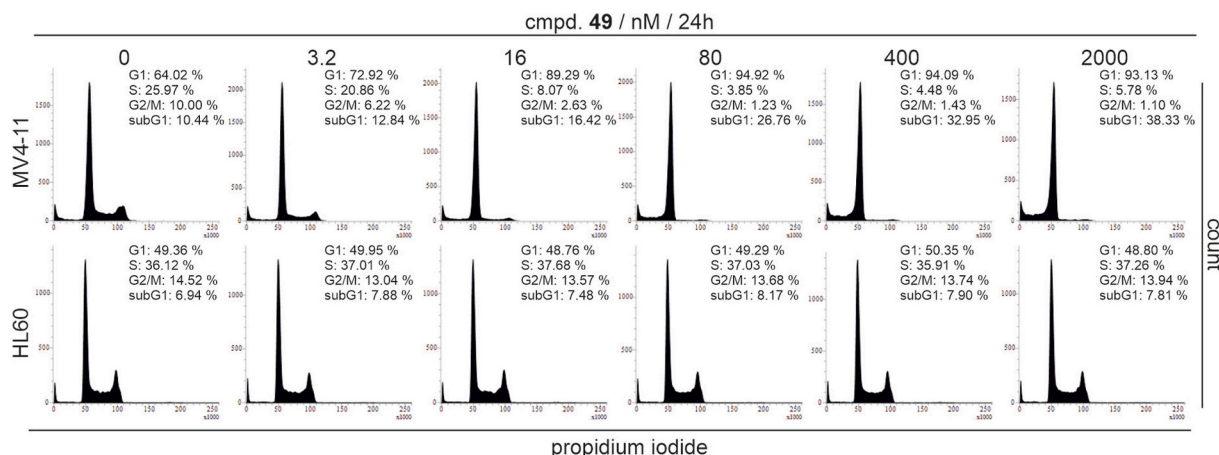


Fig. 6. Cell cycle analysis of MV4-11 and HL60 cells treated with 49 for 24 h.

quizartinib, used as standards (Table 2). The cell lines were selected to further assess the selectivity of 49.

FLT3, together with PDGFR, CSF1R, and KIT, belongs to the type III RTKs, and the close relationship between these kinases often results in simultaneous inhibition of these targets by the known FLT3 inhibitors, which can sometimes be very problematic. Simultaneous inhibition of FLT3 and KIT has been shown to induce myelosuppression [43], which complicates the clinical use of such compounds. Therefore, the high selectivity ratio between FLT3 and KIT is discussed as an advantage [19]. For further evaluation of the antiproliferative activities of compound 49, the Kasumi-1 and EOL-1 cell lines were selected (Table 2). Kasumi-1 is characterized by the presence of an N822K activating mutation in the *KIT* gene, and compound-induced inhibition of Kasumi-1 proliferation usually corresponds to the KIT-inhibitory properties of the molecule. The EOL-1 cell line is characterized by the presence of the *FIP1L1-PDGFR* fusion gene, which results in the loss of the auto-inhibitory function of PDGFR. As with Kasumi-1, inhibition of EOL-1 proliferation can often be linked to PDGFR inhibition induced by treatment.

Compound 49, as well as sorafenib and quizartinib used as standards, showed nanomolar potency against EOL-1, suggesting potent inhibition of PDGFR. More importantly, the potency of 49 against Kasumi-1 varied in the micromolar range (Table 2). The low sensitivity of this cell line to the treatment suggests that compound 49, unlike sorafenib and quizartinib, is not a potent inhibitor of KIT kinase, making this structural motif interesting for further development.

As previously mentioned, another common challenge in FLT3 inhibitor therapy is the development of resistance due to secondary mutations in the FLT3 gene. Thus, the Ba/F3 cellular model including FLT3-ITD and FLT3-ITD-F691L stably-transfected cells was selected in the present study. As shown in Table 2, the nanomolar activity of compound 49 against Ba/F3-FLT3-ITD further confirmed its FLT3-dependent mechanism of action. Interestingly, 49 retained promising efficacy also against Ba/F3-FLT3-ITD-F691L cells, which are more than 35 times more sensitive to the treatment than parental Ba/F3 cells. The F691L secondary mutation in FLT3-ITD dramatically limits the use of most known FLT3 inhibitors, as it significantly reduces their efficacy [44,45]. The slight decrease in potency of 49 against FLT3-ITD-F691L positive cells compared to FLT3-ITD cells is consistent with results from assays with recombinant enzymes. While the IC_{50} value against FLT3-ITD is 0.031 μ M (Table 1), the potency against FLT3-ITD-F691L was

approximately eight times lower ($IC_{50} = 0.239 \pm 0.006 \mu$ M). A more pronounced difference in potency was observed using quizartinib (the GI_{50} values for Ba/F3 FLT3-ITD and FLT3-ITD-F691L cells were 0.003 and 0.502 μ M, respectively; the IC_{50} values obtained using recombinant enzymes were 0.030 μ M for FLT3-ITD and $>1 \mu$ M for FLT3-ITD-F691L).

The ability of 49 to reduce FLT3 autophosphorylation and block its downstream signaling pathways was also confirmed by immunoblotting analysis. Although 49 was approximately five times more potent in Ba/F3 FLT3-ITD cells than in Ba/F3 FLT3-ITD-F691L cells (Fig. 8), this potency is still comparable to MV4-11 FLT3-ITD cells (Fig. 7). The decrease in sensitivity of Ba/F3 cells expressing FLT3-ITD-F691L to quizartinib observed in the parallel control experiment was even more pronounced (Fig. S2).

3. Conclusion

In conclusion, this study emphasizes the imperative of addressing FLT3 mutations in the pursuit of enhanced therapeutic strategies for AML. The complex landscape of AML pathogenesis, coupled with the significant prevalence of FLT3 mutations, demands innovative therapeutic interventions. The evolution from first to second generation FLT3 inhibitors reflects the ongoing quest for selectivity and potency.

This study introduces a novel series of furo[2,3-*d*]pyrimidin-1,3,4-thiadiazole-urea derivatives, demonstrating remarkable FLT3-ITD inhibitory activity. Comprehensive investigations revealed promising selectivity of the novel compounds against FLT3-ITD-expressing hematological cell lines.

Based on these data, compound 49 was further evaluated as a promising candidate. Notably, its effectiveness extend to the suppression of FLT3 phosphorylation along with the downstream signaling pathways. The results of the cell viability assay against Ba/F3 FLT3-mutant cell lines showed that compound 49 exhibited potent effects, particularly against the Ba/F3 FLT3-ITD-F691L cell line, surpassing sorafenib and quizartinib as reference drugs. Molecular docking study indicated that compound 49 binds to the active site of FLT3 with the same pattern as quizartinib, characterized by the accommodation of the furo-pyrimidine in the hinge region and the urea moiety in the DFG pocket of the inactive form of FLT3.

Overall, we have identified the suitability of the furo[2,3-*d*]pyrimidin-1,3,4-thiadiazole-urea backbone to contribute to the expanding landscape of FLT3-targeted therapy for AML treatment as potential drug

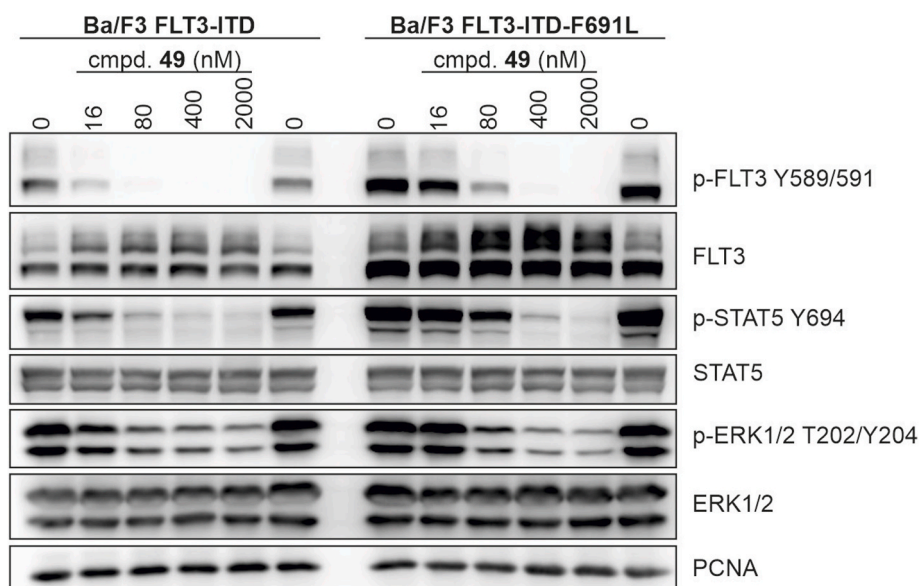


Fig. 8. Immunoblotting analysis of the phosphorylation status of FLT3 and its downstream targets in Ba/F3 FLT3-ITD and Ba/F3 FLT3-ITD-F691L cells treated with 49 for 2 h.

candidates.

4. Experimental section

4.1. General chemistry

All starting materials, reagents, and solvents were purchased from Merck and Sigma Aldrich companies without any purification. The reaction progress and the purity of synthesized compounds were monitored by thin-layer chromatography (TLC) on silica gel 250- μm F254 plastic sheets; zones were detected visually under UV light (254 nm). Chromatography columns were prepared by using 230–400 mesh silica gel and the indicated solvent system. The melting points were determined by Electrothermal IA9100 apparatus. IR spectra were obtained on PerkinElmer Spectrum Version 10.03.06 (potassium bromide disks). Elemental analyses for C, H, and N were performed using a Heraeus CHN–O–Rapid analyzer. HRMS analysis was performed using a Waters Synapt G1 HDMS High Definition mass spectrometer equipped with an electrospray ionization (ESI) source. The samples were prepared by diluting the isolated compounds in methanol to a final concentration of 10 $\mu\text{g}/\text{mL}$. The analysis was conducted mainly in negative ion mode with a mass range of m/z 50–1000. ^1H and ^{13}C NMR spectra were measured (DMSO- d_6 solution) with Bruker DRX-300 (at 300.1 and 75.5 MHz) and Bruker DRX-500 AVANCE (at 500.1 and 125.1 MHz) instruments. Chemical shifts were reported in parts per million (ppm), downfield from tetramethylsilane. Proton coupling patterns were described as singlet (s), doublet (d), triplet (t), multiplet (m), and broad (br.). The chromatographic purity of the compounds was determined using HPLC-UV and was always at least 95 %; chromatograms are available from the supplementary information.

4.2. General experimental procedures

4.2.1. General procedure for the preparation of 5-amino-1,3,4-thiadiazole-2-thiol (**2**)

Thiosemicarbazide **1** (1 equiv.) and Na_2CO_3 (1 equiv.) were dissolved in dry ethanol, and the mixture was heated to 60 $^\circ\text{C}$ for 30 min. Afterwards, a solution of carbon disulfide (2 equiv.) in dry EtOH was added dropwise, and the resultant mixture was refluxed overnight. When the completion of the reaction was detected by TLC analysis, the solvent was evaporated under reduced pressure. The residue was diluted using water and then acidified using concentrated HCl solution to obtain 5-amino-1,3,4-thiadiazole-2-thiol **2** (in 84 % yield) as yellow precipitate.

4.2.2. General procedure for the preparation of 1-(5-mercapto-1,3,4-thiadiazol-2-yl)-3-arylurea derivatives (**3–16**)

A solution of compound **2** (1 equiv.) in dry DCM under an argon atmosphere was stirred at room temperature for 30 min. Subsequently, desired phenyl isocyanate derivative (1 equiv.) was added to the mixture, and stirring continued overnight. Once the reaction was complete, a solid residue precipitated. Finally, the white precipitate was filtered to obtain corresponding diarylurea derivatives **3–16**. Each product was used for the next step without any further purification.

4.2.3. Synthetic procedure for the preparation of *N*-(5-mercapto-1,3,4-thiadiazol-2-yl)benzamide (**17**)

Initially, a solution of benzoic acid (1 mmol) in excess amount of thionyl chloride (SOCl_2) was heated under reflux conditions for 2 h. After completion of the reaction, as identified by TLC, the remaining part of SOCl_2 was removed under vapor pressure to isolate the desired benzoyl chloride, which was sufficiently pure to be used directly for further step.

In the second step, to the stirring solution of 5-amino-1,3,4-thiadiazole-2-thiol **2** (1 mmol) and Et_3N (1.2 mmol) in dry DMF under an argon atmosphere at room temperature, freshly synthesized benzoyl chloride

was added, and resulting mixture was stirred at the same temperature for 12 h. Upon confirming the completion of the reaction through TLC analysis, the mixture was quenched in the water bath containing crushed ice, and the precipitated product was filtered and washed with Et_2O to afford pure *N*-(5-mercapto-1,3,4-thiadiazol-2-yl)benzamide **17** (in 78 % yield) in the form of a white powder.

4.2.4. Synthetic procedure for the preparation of 2-amino-4,5-diphenylfuran-3-carbonitrile (**19**)

To a mixture of benzoin **18** (1 equiv.) and malononitrile (1.8 equiv.) in DMF under the ice-bath conditions at 0 $^\circ\text{C}$, Et_2NH (1 equiv.) was added dropwise over a period of 30 min. Subsequently, the resulting mixture was stirred at room temperature for 24 h. Once the starting materials finished as checked by TLC analysis, water was added to the reaction mixture to precipitate the desirable poly-substituted furan **19**. This precipitate was then filtered and washed with *n*-hexane. Finally, 2-amino-4,5-diphenylfuran-3-carbonitrile **19** was obtained in 69 % yield as pure brown powder.

4.2.5. Synthetic procedure for the preparation of 2-amino-5-phenylfuran-3-carbonitriles (**40**)

A mixture of phenacylbromide **37** (1 equiv.), malononitrile (1.3 equiv.), and Et_2NH (1 equiv.) in DMF at room temperature was stirred for 16 h. After completion of the reaction upon TLC analysis, water was added to the mixture to precipitate the desired product, which was filtered, washed with Et_2O , and recrystallized using EtOH to give pure product **40** in a 74 % yield.

4.2.6. Synthetic procedure for the preparation of 2-amino-5-(4-methoxyphenyl)furan-3-carbonitrile (**41**)

To afford this compound, it was necessary to synthesize and isolate 2-(2-(4-methoxyphenyl)-2-oxoethyl)malononitrile **39** (as a key intermediate), followed by its conversion into the furan backbone. To this goal, a mixture of 4-methoxy phenacylbromide **38** (1 equiv.), malononitrile (1.2 equiv.), and NaOH in EtOH was stirred on ice for 30 min. Upon complete consumption of compound **38**, as confirmed by TLC, the resulting mixture was concentrated, and obtained white crude was immediately used for next steps without further purification. Subsequent steps of synthetic protocol were similar to that described for the preparation of compound **40** (the yield was 40 %).

4.2.7. General procedure for the preparation of substituted furo[2,3-*d*]pyrimidin-4(3*H*)-ones (**20**, **42**, and **43**)

The corresponding substituted 2-aminofuran-3-carbonitrile (1 equiv.) was dissolved in formic acid (3 equiv.), and then acetic anhydride (3 equiv.) was slowly added dropwise at 0 $^\circ\text{C}$ over a period of 20 min. The reaction mixture was stirred at room temperature for 1 h and subsequently refluxed for 16 h. After confirming the completion of the reaction using TLC analysis, cold water was added to the reaction mixture, and the brown resulting precipitate was filtered and washed thoroughly with water to afford pure desired products. It must be noted that the time reaction for the preparation of compounds **42** and **43** was almost 24 h.

4.2.8. General procedure for the preparation of 4-chlorofuro[2,3-*d*]pyrimidines (**21**, **44**, and **45**)

To the balloon containing compound **20**, **42**, or **43** (1 equiv.), kept on ice, phosphorus trichloride (POCl_3) (1.2 equiv.) was added dropwise. The reaction mixture was stirred at room temperature for 30 min and subsequently refluxed for 2 h. Afterwards, the solution was extracted three times with water and EtOAc. The combined organic extracts were washed with brine, dried over Na_2SO_4 , and then concentrated. The residue was purified by column chromatography using *n*-hexane/EtOAc (3:7) as eluent, resulting in the corresponding pure products.

4.2.9. General procedure for the preparation of targeted substituted furo [2,3-d]pyrimidine derivatives (21, 44, and 45)

After a solution of desired substituted 1,3,4-thiadiazole-urea derivatives 3–16 (1 equiv.) and Et₃N (1.2 equiv.) in EtOH was heated under reflux conditions for 30 min, the corresponding substituted 4-chlorofuro[2,3-d]pyrimidine derivatives 21, 44, or 45 (1 equiv.) were added gradually to the reaction mixture, stirring continued for 24 h. Upon completion of reaction (using TLC monitoring), the mixture was cooled to ambient temperature, and the solid residue precipitated during 30 min. The precipitate was filtered and washed with EtOH to obtain corresponding pure product in the form of a milky powder with great to excellent yields. The appropriate solvent for the reaction between compounds 17 and 21 to afford product 36 was CH₃CN.

4.2.9.1. 1-(5-((5,6-diphenylfuro[2,3-d]pyrimidin-4-yl)thio)-1,3,4-thiadiazol-2-yl)-3-phenylurea (22). White solid, mp: 269–271 °C, yield: 79 %. IR (KBr) ($\nu_{\max}/\text{cm}^{-1}$): 3389 and 2924 (2NH), 1707 (C=O), 1578, 1538, 1501, 1437, 1386, 1312, 1241, 1206, 1156, 1071, 1028, 980, 768, 749, 698, 643. ¹H NMR (300.1 MHz, DMSO-*d*₆): δ 11.18 (s, 1H, NH), 9.01 (s, 1H, NH), 8.83 (s, 1H, CH), 7.65–7.57 (m, 5H, 5CH), 7.55–7.49 (m, 2H, 2CH), 7.48 (d, *J* = 7.9 Hz, 2H, 2CH), 7.43–7.36 (m, 3H, 3CH), 7.32 (t, *J* = 7.7 Hz, 2H, 2CH), 7.06 (t, *J* = 7.3 Hz, 1H, CH). ¹³C NMR (75.1 MHz, DMSO-*d*₆): δ 163.81, 157.75, 153.13, 150.26, 138.58, 130.95, 130.72, 130.31, 129.92, 129.69, 129.38, 128.55, 127.01, 123.68, 119.40, 117.65, 115.44. Anal. Calcd. for C₂₇H₁₈N₆O₂S₂: C, 62.05; H, 3.47; N, 16.08; found: C, 62.38; H, 3.69; N, 16.32 %. HRMS (ESI) *m/z* for C₂₇H₁₇N₆O₂S₂[−] [M – H][−], calculated: 521.0854, found: 521.0876. HPLC purity: 98.81 % (t_R = 14.79 min).

4.2.9.2. 1-(5-((5,6-diphenylfuro[2,3-d]pyrimidin-4-yl)thio)-1,3,4-thiadiazol-2-yl)-3-(3-tolyl)urea (23). White solid, mp: 248–251 °C, yield: 62 %. IR (KBr) ($\nu_{\max}/\text{cm}^{-1}$): 3395 and 2981 (2NH), 1694 (C=O), 1616, 1583, 1538, 1489, 1447, 1429, 1417, 1388, 1304, 1262, 1245, 1211, 979, 785, 746, 700, 685. ¹H NMR (500.1 MHz, DMSO-*d*₆): δ 11.13 (s, 1H, NH), 9.00 (s, 1H, NH), 8.81 (s, 1H, CH), 7.63–7.57 (m, 5H, 5CH), 7.54–7.50 (m, 2H, 2CH), 7.40–7.34 (m, 3H, 3CH), 7.32 (s, 1H, CH), 7.26 (d, *J* = 7.8 Hz, 1H, CH), 7.19 (t, *J* = 7.7 Hz, 1H, CH), 6.87 (d, *J* = 7.2 Hz, 1H, CH), 2.29 (s, 3H, CH₃). ¹³C NMR (125.1 MHz, DMSO-*d*₆): δ 163.86, 157.62, 153.18, 150.28, 138.71, 138.49, 130.97, 130.73, 129.93, 129.71, 129.42, 129.39, 129.23, 128.60, 127.03, 124.44, 119.84, 117.66, 116.55, 21.60. Anal. Calcd. for C₂₈H₂₀N₆O₂S₂: C, 62.67; H, 3.76; N, 15.66; found: C, 62.43; H, 3.94; N, 15.89 %. HRMS (ESI) *m/z* for C₂₈H₁₉N₆O₂S₂[−] [M – H][−], calculated: 535.1011, found: 535.1050. HPLC purity: 98.17 % (t_R = 14.83 min).

4.2.9.3. 1-(5-((5,6-diphenylfuro[2,3-d]pyrimidin-4-yl)thio)-1,3,4-thiadiazol-2-yl)-3-(4-tolyl)urea (24). White solid, mp: 277–279 °C, yield: 68 %. IR (KBr) ($\nu_{\max}/\text{cm}^{-1}$): 3376 and 2918 (2NH), 1708 (C=O), 1577, 1537, 1447, 1385, 1312, 1242, 1204, 1156, 1066, 1029, 980, 815, 766, 696, 602. ¹H NMR (300.1 MHz, DMSO-*d*₆): δ 11.08 (s, 1H, NH), 8.94 (s, 1H, NH), 8.75 (s, 1H, CH), 8.00–6.88 (m, 14H, 14CH), 2.20 (s, 3H, CH₃). Anal. Calcd. for C₂₈H₂₀N₆O₂S₂: C, 62.67; H, 3.76; N, 15.66; found: C, 62.85; H, 3.89; N, 15.54 %. HRMS (ESI) *m/z* for C₂₈H₁₉N₆O₂S₂[−] [M – H][−], calculated: 535.1011, found: 535.0979. HPLC purity: 96.57 % (t_R = 14.78 min).

4.2.9.4. 1-(5-((5,6-diphenylfuro[2,3-d]pyrimidin-4-yl)thio)-1,3,4-thiadiazol-2-yl)-3-(3-methoxyphenyl)urea (25). White solid, mp: 261–263 °C, yield: 71 %. IR (KBr) ($\nu_{\max}/\text{cm}^{-1}$): 3374 and 2962 (2NH), 1624 (C=O), 1579, 1543, 1496, 1465, 1447, 1353, 1295, 1245, 1215, 1169, 1156, 1028, 980, 770, 699, 686. ¹H NMR (300.1 MHz, DMSO-*d*₆): δ 11.30 (s, 1H, NH), 10.09 (s, 1H, NH), 8.81 (s, 1H, CH), 7.65–7.57 (m, 5H, 5CH), 7.54 (dd, *J* = 7.3, 2.4 Hz, 2H, 2CH), 7.42–7.34 (m, 3H, 3CH), 7.28 (s, 1H, CH), 7.22–7.10 (m, 2H, 2CH), 6.58 (dd, *J* = 8.8, 2.1 Hz, 1H, CH), 3.72 (s, 3H, CH₃). ¹³C NMR (75.1 MHz, DMSO-*d*₆): δ 163.35,

159.66, 157.91, 153.34, 152.77, 149.73, 147.33, 140.23, 130.61, 130.34, 129.83, 129.61, 129.32, 128.93, 128.15, 126.61, 117.18, 115.06, 104.26, 45.75. Anal. Calcd. for C₂₈H₂₀N₆O₃S₂: C, 60.85; H, 3.65; N, 15.21; found: C, 61.04; H, 3.85; N, 15.44 %. HRMS (ESI) *m/z* for C₂₈H₁₉N₆O₃S₂[−] [M – H][−], calculated: 551.0960, found: 551.0979. HPLC purity: 99.24 % (t_R = 15.21 min).

4.2.9.5. 1-(5-((5,6-diphenylfuro[2,3-d]pyrimidin-4-yl)thio)-1,3,4-thiadiazol-2-yl)-3-(4-methoxyphenyl)urea (26). White solid, mp: 298–300 °C, yield: 74 %. IR (KBr) ($\nu_{\max}/\text{cm}^{-1}$): 3385 and 2953 (2NH), 1710 (C=O), 1594, 1578, 1544, 1513, 1466, 1419, 1388, 1317, 1249, 1207, 1186, 1174, 1157, 981, 825, 699. ¹H NMR (500.1 MHz, DMSO-*d*₆): δ 11.11 (s, 1H, NH), 8.91 (s, 1H, NH), 8.80 (s, 1H, CH), 7.62–7.55 (m, 5H, 5CH), 7.54–7.48 (m, 2H, 2CH), 7.41–7.33 (m, 5H, 5CH), 6.89 (d, *J* = 7.8 Hz, 2H, 2CH), 3.71 (s, 3H, OCH₃). ¹³C NMR (125.1 MHz, DMSO-*d*₆): δ 163.83, 157.88, 155.88, 153.16, 150.26, 130.96, 130.73, 130.32, 129.92, 129.70, 129.40, 128.57, 127.02, 121.40, 117.67, 115.47, 114.53, 55.66. Anal. Calcd. for C₂₈H₂₀N₆O₃S₂: C, 60.85; H, 3.65; N, 15.21; found: C, 61.08; H, 3.91; N, 15.04 %. HRMS (ESI) *m/z* for C₂₈H₁₉N₆O₃S₂[−] [M – H][−], calculated: 551.0960, found: 551.0947. HPLC purity: 98.22 % (t_R = 15.29 min).

4.2.9.6. 1-(5-((5,6-diphenylfuro[2,3-d]pyrimidin-4-yl)thio)-1,3,4-thiadiazol-2-yl)-3-(3-fluorophenyl)urea (27). White solid, mp: 282–285 °C, yield: 58 %. IR (KBr) ($\nu_{\max}/\text{cm}^{-1}$): 3389 and 2972 (2NH), 1699 (C=O), 1532, 1522, 1478, 1442, 1421, 1413, 1376, 1310, 1267, 1243, 1219, 960, 773, 741, 681. ¹H NMR (500.1 MHz, DMSO-*d*₆): δ 11.28 (s, 1H, NH), 9.35 (s, 1H, NH), 8.82 (s, 1H, CH), 7.73–7.28 (m, 12H, 12CH), 7.22 (s, 1H, CH), 6.87 (d, *J* = 8.6 Hz, 1H, CH). ¹³C NMR (125.1 MHz, DMSO-*d*₆): δ 163.86, 162.74 (¹*J*_{C-F} = 240.2 Hz), 157.77, 153.21, 150.29, 138.95, 131.07, 130.74, 130.38, 129.97, 129.75, 129.46, 128.59, 127.05, 117.74, 116.89, 115.36 (²*J*_{C-F} = 25.9 Hz), 115.25, 106.18 (²*J*_{C-F} = 26.1 Hz). Anal. Calcd. for C₂₇H₁₇FN₆O₂S₂: C, 59.99; H, 3.17; N, 15.55; found: C, 60.15; H, 3.36; N, 15.26 %. HRMS (ESI) *m/z* for C₂₇H₁₆FN₆O₂S₂[−] [M – H][−], calculated: 539.0760, found: 539.0803. HPLC purity: 99.90 % (t_R = 15.15 min).

4.2.9.7. 1-(3-chlorophenyl)-3-(5-((5,6-diphenylfuro[2,3-d]pyrimidin-4-yl)thio)-1,3,4-thiadiazol-2-yl)urea (28). White solid, mp: 278–280 °C, yield: 72 %. IR (KBr) ($\nu_{\max}/\text{cm}^{-1}$): 3377 and 2977 (2NH), 1708 (C=O), 1591, 1584, 1538, 1482, 1447, 1407, 1399, 1298, 1232, 1210, 1070, 980, 746, 700, 687. ¹H NMR (300.1 MHz, DMSO-*d*₆): δ 11.24 (s, 1H, NH), 9.27 (s, 1H, NH), 8.77 (s, 1H, CH), 7.73–7.20 (m, 13H, 13CH), 7.05 (s, 1H, CH). ¹³C NMR (75.1 MHz, DMSO-*d*₆): δ 163.26, 156.88, 152.53, 149.77, 149.03, 139.75, 133.26, 130.43, 130.22, 129.75, 129.25, 128.81, 128.01, 126.48, 122.67, 118.37, 117.33, 117.01, 114.86. Anal. Calcd. for C₂₇H₁₇ClN₆O₂S₂: C, 58.22; H, 3.08; N, 15.09; found: C, 58.47; H, 3.26; N, 14.88 %. HRMS (ESI) *m/z* for C₂₇H₁₆ClN₆O₂S₂[−] [M – H][−], calculated: 555.0465, found: 555.0515. HPLC purity: 99.32 % (t_R = 15.20 min).

4.2.9.8. 1-(4-chlorophenyl)-3-(5-((5,6-diphenylfuro[2,3-d]pyrimidin-4-yl)thio)-1,3,4-thiadiazol-2-yl)urea (29). White solid, mp: 302–305 °C, yield: 87 %. IR (KBr) ($\nu_{\max}/\text{cm}^{-1}$): 3377, and 2982 (2NH), 1715 (C=O), 1577, 1542, 1494, 1444, 1418, 1386, 1308, 1290, 1243, 1208, 1124, 1061, 971, 960, 768, 698, 687. ¹H NMR (300.1 MHz, DMSO-*d*₆): δ 11.33 (s, 1H, NH), 9.37 (s, 1H, NH), 8.83 (s, 1H, CH), 7.65–7.58 (m, 5H, 5CH), 7.56–7.48 (m, 4H, 4CH), 7.43–7.33 (m, 5H, 5CH). ¹³C NMR (75.1 MHz, DMSO-*d*₆): δ 163.83, 157.68, 153.13, 150.28, 137.66, 130.95, 130.71, 130.33, 129.93, 129.70, 129.40, 129.22, 128.55, 127.02, 121.02, 117.67, 115.44. Anal. Calcd. for C₂₇H₁₇ClN₆O₂S₂: C, 58.22; H, 3.08; N, 15.09; found: C, 58.36; H, 3.33; N, 15.28 %. HRMS (ESI) *m/z* for C₂₇H₁₆ClN₆O₂S₂[−] [M – H][−], calculated: 555.0465, found: 555.0515. HPLC purity: 98.86 % (t_R = 15.27 min).

4.2.9.9. *1-(2-bromophenyl)-3-(5-((5,6-diphenylfuro[2,3-d]pyrimidin-4-yl)thio)-1,3,4-thiadiazol-2-yl)urea (30)*. White solid, mp: 295–298 °C, yield: 81 %. IR (KBr) ($\nu_{\max}/\text{cm}^{-1}$): 3350 and 2925 (2NH), 1703 (C=O), 1579, 1528, 1467, 1432, 1385, 1324, 1296, 1237, 1208, 1155, 1072, 1026, 981, 959, 748, 697. ^1H NMR (500.1 MHz, DMSO- d_6): δ 11.89 (s, 1H, NH), 8.83 (s, 1H, NH), 8.65 (s, 1H, CH), 8.02 (d, $J = 8.2$ Hz, 1H, CH), 7.64–7.48 (m, 7H, 7CH), 7.44–7.34 (m, 5H, 5CH), 7.08 (t, $J = 7.6$ Hz, 1H, CH). ^{13}C NMR (125.1 MHz, DMSO- d_6): δ 163.85, 157.72, 153.18, 150.29, 136.17, 133.17, 130.99, 130.74, 130.39, 129.98, 129.75, 129.69, 129.46, 128.79, 128.59, 127.04, 126.10, 117.72, 115.49. Anal. Calcd. for $\text{C}_{27}\text{H}_{17}\text{BrN}_6\text{O}_2\text{S}_2$: C, 53.91; H, 2.85; N, 13.97; found: C, 54.12; H, 3.16; N, 14.19 %. HRMS (ESI) m/z for $\text{C}_{27}\text{H}_{16}\text{BrN}_6\text{O}_2\text{S}_2^-$ [$\text{M} - \text{H}$] $^-$, calculated: 598.9960, found: 599.0012. HPLC purity: 99.61 % ($t_{\text{R}} = 15.30$ min).

4.2.9.10. *1-(4-bromophenyl)-3-(5-((5,6-diphenylfuro[2,3-d]pyrimidin-4-yl)thio)-1,3,4-thiadiazol-2-yl)urea (31)*. White solid, mp: 316–319 °C, yield: 92 %. IR (KBr) ($\nu_{\max}/\text{cm}^{-1}$): 3385 and 2972 (2NH), 1714 (C=O), 1590, 1578, 1532, 1491, 1450, 1427, 1389, 1328, 1290, 1241, 1180, 1156, 980, 828, 767, 687. ^1H NMR (300.1 MHz, DMSO- d_6): δ 11.24 (s, 1H, NH), 9.25 (s, 1H, NH), 8.81 (s, 1H, CH), 7.80–7.15 (m, 14H, 14CH). ^{13}C NMR (75.1 MHz, DMSO- d_6): δ 163.82, 157.65, 153.13, 150.28, 138.32, 132.12, 130.95, 130.71, 130.33, 129.93, 129.70, 129.40, 128.55, 127.02, 121.37, 117.67, 115.44. Anal. Calcd. for $\text{C}_{27}\text{H}_{17}\text{BrN}_6\text{O}_2\text{S}_2$: C, 53.91; H, 2.85; N, 13.97; found: C, 54.36; H, 3.22; N, 14.28 %. HRMS (ESI) m/z for $\text{C}_{27}\text{H}_{18}\text{BrN}_6\text{O}_2\text{S}_2^+$ [$\text{M} + \text{H}$] $^+$, calculated: 601.0111, found: 601.0109. HPLC purity: 99.37 % ($t_{\text{R}} = 15.30$ min).

4.2.9.11. *1-(3-chloro-4-methylphenyl)-3-(5-((5,6-diphenylfuro[2,3-d]pyrimidin-4-yl)thio)-1,3,4-thiadiazol-2-yl)urea (32)*. White solid, mp: 297–299 °C, yield: 73 %. IR (KBr) ($\nu_{\max}/\text{cm}^{-1}$): 3383 and 2931 (2NH), 1717 (C=O), 1578, 1537, 1499, 1446, 1426, 1418, 1387, 1300, 1244, 1205, 1072, 1051, 980, 835, 768, 698, 687. ^1H NMR (500.1 MHz, DMSO- d_6): δ 11.26 (s, 1H, NH), 9.20 (s, 1H, NH), 8.84 (s, 1H, CH), 7.68 (s, 1H, CH), 7.66–7.50 (m, 9H, 9CH), 7.45–7.37 (m, 3H, 3CH), 7.30–7.24 (m, 2H, 2CH), 2.27 (s, 3H, CH $_3$). Anal. Calcd. for $\text{C}_{27}\text{H}_{19}\text{ClN}_6\text{O}_2\text{S}_2$: C, 58.01; H, 3.43; N, 15.03; found: C, 57.83; H, 3.66; N, 15.28 %. HRMS (ESI) m/z for $\text{C}_{27}\text{H}_{18}\text{ClN}_6\text{O}_2\text{S}_2^-$ [$\text{M} - \text{H}$] $^-$, calculated: 569.0621, found: 569.0611. HPLC purity: 98.93 % ($t_{\text{R}} = 17.10$ min).

4.2.9.12. *1-(2,4-difluorophenyl)-3-(5-((5,6-diphenylfuro[2,3-d]pyrimidin-4-yl)thio)-1,3,4-thiadiazol-2-yl)urea (33)*. White solid, mp: 287–290 °C, yield: 80 %. IR (KBr) ($\nu_{\max}/\text{cm}^{-1}$): 3373 and 2896 (2NH), 1719 (C=O), 1602, 1579, 1548, 1505, 1456, 1429, 1398, 1386, 1326, 1261, 1215, 1198, 1143, 1104, 979, 961, 846, 699. ^1H NMR (500.1 MHz, DMSO- d_6): δ 11.43 (s, 1H, NH), 8.97 (s, 1H, NH), 8.84 (s, 1H, CH), 7.66–7.59 (m, 5H, 5CH), 7.57–7.50 (m, 2H, 2CH), 7.44–7.33 (m, 5H, 5CH), 7.11 (t, $J = 7.8$ Hz, 1H, CH). ^{13}C NMR (125.1 MHz, DMSO- d_6): δ 163.85, 162.38 ($^1J_{\text{C-F}} = 200.4$ Hz), 162.00 ($^1J_{\text{C-F}} = 198.9$ Hz), 157.67, 153.17, 150.29, 136.27, 130.98, 130.73, 130.39, 129.98, 129.75, 129.46, 128.58, 127.04, 117.71, 115.48, 111.83 ($^2J_{\text{C-F}} = 18.7$ Hz), 104.51 ($^2J_{\text{C-F}} = 26.8$ Hz). Anal. Calcd. for $\text{C}_{27}\text{H}_{16}\text{F}_2\text{N}_6\text{O}_2\text{S}_2$: C, 58.06; H, 2.89; N, 15.05; found: C, 58.32; H, 3.08; N, 14.89 %. HRMS (ESI) m/z for $\text{C}_{27}\text{H}_{15}\text{F}_2\text{N}_6\text{O}_2\text{S}_2^-$ [$\text{M} - \text{H}$] $^-$, calculated: 557.0666, found: 557.0659. HPLC purity: 98.89 % ($t_{\text{R}} = 15.28$ min).

4.2.9.13. *1-(3,4-dichlorophenyl)-3-(5-((5,6-diphenylfuro[2,3-d]pyrimidin-4-yl)thio)-1,3,4-thiadiazol-2-yl)urea (34)*. White solid, mp: 278–281 °C, yield: 78 %. IR (KBr) ($\nu_{\max}/\text{cm}^{-1}$): 3380 and 2924 (2NH), 1719 (C=O), 1578, 1535, 1477, 1454, 1427, 1386, 1334, 1298, 1232, 1206, 1155, 1136, 1073, 1028, 981, 887, 745, 699, 685. ^1H NMR (300.1 MHz, DMSO- d_6): δ 11.45 (s, 1H, NH), 9.45 (s, 1H, NH), 8.84 (s, 1H, CH), 7.66–7.50 (m, 8H, 8CH), 7.47–7.34 (m, 4H, 4CH). Anal. Calcd. for $\text{C}_{27}\text{H}_{16}\text{Cl}_2\text{N}_6\text{O}_2\text{S}_2$: C, 58.06; H, 2.89; N, 15.05; found: C, 58.32; H, 3.03; N, 15.32 %. HRMS (ESI) m/z for $\text{C}_{27}\text{H}_{15}\text{Cl}_2\text{N}_6\text{O}_2\text{S}_2^-$ [$\text{M} - \text{H}$] $^-$, calculated:

589.0075, found: 589.0045. HPLC purity: 98.73 % ($t_{\text{R}} = 17.13$ min).

4.2.9.14. *1-(4-chloro-3-(trifluoromethyl)phenyl)-3-(5-((5,6-diphenylfuro[2,3-d]pyrimidin-4-yl)thio)-1,3,4-thiadiazol-2-yl)urea (35)*. White solid, mp: 287–290 °C, yield: 80 %. IR (KBr) ($\nu_{\max}/\text{cm}^{-1}$): 3378 and 2913 (2NH), 1716 (C=O), 1596, 1576, 1542, 1486, 1445, 1391, 1317, 1237, 1213, 1187, 1181, 1114, 980, 823, 747, 700. ^1H NMR (300.1 MHz, DMSO- d_6): δ 11.52 (s, 1H, NH), 9.60 (s, 1H, NH), 8.84 (s, 1H, CH), 8.08 (s, 1H, CH), 7.75 (t, $J = 7.8$ Hz, 1H, CH), 7.67 (s, 1H, CH), 7.66–7.57 (m, 5H, 5CH), 7.56–7.48 (m, 2H, 2CH), 7.43–7.36 (m, 3H, 3CH). Anal. Calcd. for $\text{C}_{28}\text{H}_{16}\text{ClF}_3\text{N}_6\text{O}_2\text{S}_2$: C, 53.80; H, 2.58; N, 13.45; found: C, 53.92; H, 2.50; N, 13.63 %. HRMS (ESI) m/z for $\text{C}_{27}\text{H}_{15}\text{Cl}_2\text{N}_6\text{O}_2\text{S}_2^-$ [$\text{M} - \text{H}$] $^-$, calculated: 623.0339, found: 623.0316. HPLC purity: 98.80 % ($t_{\text{R}} = 17.16$ min).

4.2.9.15. *N-(5-((5,6-diphenylfuro[2,3-d]pyrimidin-4-yl)thio)-1,3,4-thiadiazol-2-yl)benzamide (36)*. White solid, mp: 248–250 °C, yield: 48 %. IR (KBr) ($\nu_{\max}/\text{cm}^{-1}$): 3268 (NH), 1659 (C=O), 1580, 1540, 1520, 1495, 1445, 1427, 1417, 1386, 1298, 1254, 1207, 1076, 980, 768, 709, 674. ^1H NMR (500.1 MHz, DMSO- d_6): δ 13.29 (s, 1H, NH), 8.86 (s, 1H, CH), 8.13 (d, $J = 7.8$ Hz, 2H, 2CH), 7.65–7.50 (m, 9H, 9CH), 7.35–7.45 (m, 3H, 3CH). Anal. Calcd. for $\text{C}_{27}\text{H}_{17}\text{N}_5\text{O}_2\text{S}_2$: C, 62.05; H, 3.28; N, 13.40; found: C, 62.27; H, 3.42; N, 13.58 %. HRMS (ESI) m/z for $\text{C}_{27}\text{H}_{16}\text{N}_5\text{O}_2\text{S}_2^-$ [$\text{M} - \text{H}$] $^-$, calculated: 506.0745, found: 506.0769. HPLC purity: 99.28 % ($t_{\text{R}} = 15.41$ min).

4.2.9.16. *1-phenyl-3-(5-((6-phenylfuro[2,3-d]pyrimidin-4-yl)thio)-1,3,4-thiadiazol-2-yl)urea (46)*. White solid, mp: 231–233 °C, yield: 71 %. IR (KBr) ($\nu_{\max}/\text{cm}^{-1}$): 3370 and 2889 (2NH), 1719 (C=O), 1580, 1551, 1502, 1490, 1443, 1429, 1371, 1328, 1317, 1257, 1202, 1081, 970, 855, 756, 685. ^1H NMR (500.1 MHz, DMSO- d_6): δ 11.48 (s, 1H, NH), 9.39 (s, 1H, NH), 8.79 (s, 1H, CH), 7.98 (d, $J = 7.3$ Hz, 2H, 2CH), 7.65 (s, 1H, CH), 7.60–7.40 (m, 5H, 5CH), 7.31 (t, $J = 7.8$ Hz, 2H, 2CH), 7.03 (t, $J = 7.4$ Hz, 1H, CH). Anal. Calcd. for $\text{C}_{21}\text{H}_{14}\text{N}_6\text{O}_2\text{S}_2$: C, 56.49; H, 3.16; N, 18.82; found: C, 56.68; H, 3.32; N, 19.04 %. HRMS (ESI) m/z for $\text{C}_{21}\text{H}_{13}\text{N}_6\text{O}_2\text{S}_2^-$ [$\text{M} - \text{H}$] $^-$, calculated: 445.0541, found: 445.0578. HPLC purity: 98.66 % ($t_{\text{R}} = 13.79$ min).

4.2.9.17. *1-(5-((6-phenylfuro[2,3-d]pyrimidin-4-yl)thio)-1,3,4-thiadiazol-2-yl)-3-(3-tolyl)urea (47)*. White solid, mp: 220–222 °C, yield: 57 %. IR (KBr) ($\nu_{\max}/\text{cm}^{-1}$): 3367 and 2922 (2NH), 1706 (C=O), 1585, 1554, 1490, 1456, 1429, 1369, 1311, 1300, 1255, 1216, 968, 834, 776, 758, 683. ^1H NMR (500.1 MHz, DMSO- d_6): δ 11.29 (s, 1H, NH), 9.07 (s, 1H, NH), 8.79 (s, 1H, CH), 7.97 (d, $J = 7.2$ Hz, 2H, 2CH), 7.65 (s, 1H, CH), 7.54 (t, $J = 7.4$ Hz, 2H, 2CH), 7.48 (d, $J = 7.3$ Hz, 1H, CH), 7.32 (s, 1H, CH), 7.26 (d, $J = 8.3$ Hz, 2H, 2CH), 7.18 (t, $J = 7.8$ Hz, 1H, CH), 6.86 (d, $J = 7.4$ Hz, 1H, CH), 2.27 (s, 3H, CH $_3$). ^{13}C NMR (125.1 MHz, DMSO- d_6): δ 165.37, 158.95, 157.30, 155.84, 153.20, 138.85, 138.67, 132.67, 130.88, 129.84, 129.38, 128.51, 125.94, 124.55, 119.98, 117.62, 116.68, 98.86, 21.74. Anal. Calcd. for $\text{C}_{22}\text{H}_{16}\text{N}_6\text{O}_2\text{S}_2$: C, 57.38; H, 3.50; N, 18.25; found: C, 57.64; H, 3.66; N, 18.58 %. HRMS (ESI) m/z for $\text{C}_{22}\text{H}_{15}\text{N}_6\text{O}_2\text{S}_2^-$ [$\text{M} - \text{H}$] $^-$, calculated: 459.0698, found: 459.0730. HPLC purity: 99.00 % ($t_{\text{R}} = 14.15$ min).

4.2.9.18. *1-(3-methoxyphenyl)-3-(5-((6-phenylfuro[2,3-d]pyrimidin-4-yl)thio)-1,3,4-thiadiazol-2-yl)urea (48)*. White solid, mp: 226–228 °C, yield: 61 %. IR (KBr) ($\nu_{\max}/\text{cm}^{-1}$): 3389 and 2924 (2NH), 1723 (C=O), 1554, 1489, 1449, 1428, 1399, 1369, 1328, 1296, 1275, 1221, 1162, 1141, 976, 858, 751, 682. ^1H NMR (500.1 MHz, DMSO- d_6): δ 11.27 (s, 1H, NH), 9.21 (s, 1H, NH), 8.76 (s, 1H, CH), 7.93 (d, $J = 6.9$ Hz, 2H, 2CH), 7.56 (s, 1H, CH), 7.53–7.47 (m, 2H, 2CH), 7.45 (d, $J = 7.0$ Hz, 1H, CH), 7.19 (t, $J = 8.0$ Hz, 1H, CH), 7.15 (s, 1H, CH), 6.99 (d, $J = 7.2$ Hz, 1H, CH), 6.61 (d, $J = 7.9$ Hz, 1H, CH), 3.72 (s, 3H, OCH $_3$). ^{13}C NMR (125.1 MHz, DMSO- d_6): δ 165.34, 160.30, 157.27, 155.81, 153.16, 151.98, 149.18, 139.97, 130.83, 130.34, 129.79, 128.48, 126.04,

125.90, 117.58, 111.76, 109.21, 105.25, 98.79, 55.65. Anal. Calcd. for $C_{22}H_{16}N_6O_3S_2$: C, 55.45; H, 3.38; N, 17.64; found: C, 55.84; H, 3.23; N, 17.92 %. HRMS (ESI) m/z for $C_{22}H_{15}N_6O_3S_2^- [M - H]^-$, calculated: 475.0647, found: 475.0636. HPLC purity: 98.90 % ($t_R = 13.79$ min).

4.2.9.19. 1-(4-methoxyphenyl)-3-(5-((6-phenylfuro[2,3-d]pyrimidin-4-yl)thio)-1,3,4-thiadiazol-2-yl)urea (49). White solid, mp: 261–264 °C, yield: 69 %. IR (KBr) (ν_{max}/cm^{-1}): 3376 and 2921 (2NH), 1712 (C=O), 1581, 1556, 1514, 1490, 1428, 1415, 1370, 1324, 1253, 1205, 1188, 1170, 1046, 971, 820, 758, 692. 1H NMR (500.1 MHz, DMSO- d_6): δ 11.26 (s, 1H, NH), 8.97 (s, 1H, NH), 8.79 (s, 1H, CH), 7.98 (d, $J = 7.4$ Hz, 2H, 2CH), 7.67 (s, 1H, CH), 7.54 (t, $J = 7.3$ Hz, 2H, 2CH), 7.49 (t, $J = 7.2$ Hz, 1H, CH), 7.38 (d, $J = 8.6$ Hz, 2H, 2CH), 6.89 (d, $J = 8.6$ Hz, 2H, 2CH), 3.70 (s, 3H, OCH₃). Anal. Calcd. for $C_{22}H_{16}N_6O_3S_2$: C, 55.45; H, 3.38; N, 17.64; found: C, 55.73; H, 3.60; N, 17.86 %. ^{13}C NMR (125.1 MHz, DMSO- d_6): δ 165.38, 164.77, 157.45, 156.00, 155.81, 153.22, 151.96, 148.95, 131.57, 130.88, 129.84, 128.50, 125.92, 121.52, 117.62, 114.65, 98.86, 55.76. HRMS (ESI) m/z for $C_{22}H_{17}N_6O_3S_2^+ [M + H]^+$, calculated: 477.0798, found: 477.0803. HPLC purity: 99.69 % ($t_R = 14.11$ min).

4.2.9.20. 1-(3-fluorophenyl)-3-(5-((6-phenylfuro[2,3-d]pyrimidin-4-yl)thio)-1,3,4-thiadiazol-2-yl)urea (50). White solid, mp: 236–238 °C, yield: 51 %. IR (KBr) (ν_{max}/cm^{-1}): 3358 and 2965 (2NH), 1710 (C=O), 1580, 1556, 1497, 1490, 1448, 1426, 1314, 1270, 1255, 1208, 1178, 1149, 969, 833, 781, 757, 685. 1H NMR (500.1 MHz, DMSO- d_6): δ 10.49 (s, 1H, NH), 9.31 (s, 1H, NH), 8.74 (s, 1H, CH), 7.89 (d, $J = 7.2$ Hz, 2H, 2CH), 7.61 (d, $^3J_{H-F} = 11.8$ Hz, 1H, CH), 7.52–7.35 (m, 5H, 5CH), 7.29 (dd, $J = 7.9, 1.2$ Hz, 1H, CH), 6.78 (t, $J = 7.4$ Hz, 1H, CH). ^{13}C NMR (125.1 MHz, DMSO- d_6): δ 165.32, 162.94 ($^1J_{C-F} = 239.8$ Hz), 161.98, 157.80, 155.70, 153.12, 148.01, 141.60 ($^3J_{C-F} = 11.1$ Hz), 130.93 ($^3J_{C-F} = 9.7$ Hz), 130.73, 129.71, 128.44, 128.24, 125.98, 125.81, 117.49, 115.01, 109.47 ($^2J_{C-F} = 21.2$ Hz), 105.96 ($^2J_{C-F} = 26.3$ Hz), 98.72. Anal. Calcd. for $C_{21}H_{13}FN_6O_2S_2$: C, 54.30; H, 2.82; N, 18.09; found: C, 54.42; H, 2.99; N, 18.31 %. HRMS (ESI) m/z for $C_{21}H_{12}FN_6O_2S_2^- [M - H]^-$, calculated: 463.0447, found: 463.0422. HPLC purity: 95.65 % ($t_R = 14.09$ min).

4.2.9.21. 1-(3-chlorophenyl)-3-(5-((6-phenylfuro[2,3-d]pyrimidin-4-yl)thio)-1,3,4-thiadiazol-2-yl)urea (51). White solid, mp: 227–230 °C, yield: 68 %. IR (KBr) (ν_{max}/cm^{-1}): 3372 and 2887 (2NH), 1709 (C=O), 1585, 1567, 1550, 1529, 1479, 1446, 1423, 1366, 1326, 1297, 1269, 1122, 968, 821, 783, 766, 679. 1H NMR (500.1 MHz, DMSO- d_6): δ 12.12 (s, 1H, NH), 10.51 (s, 1H, NH), 8.79 (s, 1H, CH), 7.95 (d, $J = 7.6$ Hz, 2H, 2CH), 7.91 (s, 1H, CH), 7.56 (d, $J = 7.5$ Hz, 1H, CH), 7.54 (t, $J = 7.4$ Hz, 2H, 2CH), 7.49 (t, $J = 7.1$ Hz, 1H, CH), 7.45 (s, 1H, CH), 7.29 (t, $J = 8.0$ Hz, 1H, CH), 6.99 (d, $J = 7.5$ Hz, 1H, CH). ^{13}C NMR (125.1 MHz, DMSO- d_6): δ 165.40, 155.41, 153.14, 142.30, 133.59, 131.45, 130.73, 130.36, 129.76, 129.10, 128.45, 127.77, 125.72, 121.65, 117.94, 117.29, 117.04, 98.77. Anal. Calcd. for $C_{21}H_{13}ClN_6O_2S_2$: C, 52.44; H, 2.72; N, 17.47; found: C, 52.68; H, 2.55; N, 17.23 %. HRMS (ESI) m/z for $C_{21}H_{12}ClN_6O_2S_2^- [M - H]^-$, calculated: 479.0152, found: 479.0143. HPLC purity: 99.56 % ($t_R = 14.15$ min).

4.2.9.22. 1-(4-chlorophenyl)-3-(5-((6-phenylfuro[2,3-d]pyrimidin-4-yl)thio)-1,3,4-thiadiazol-2-yl)urea (52). White solid, mp: 270–273 °C, yield: 84 %. IR (KBr) (ν_{max}/cm^{-1}): 3374 and 2981 (2NH), 1719 (C=O), 1584, 1545, 1493, 1431, 1412, 1369, 1310, 1291, 1259, 1242, 1207, 1093, 968, 839, 753, 686. 1H NMR (500.1 MHz, DMSO- d_6): δ 11.58 (s, 1H, NH), 9.62 (s, 1H, NH), 8.81 (s, 1H, CH), 7.99 (d, $J = 7.5$ Hz, 2H, 2CH), 7.65 (s, 1H, CH), 7.60–7.53 (m, 3H, 3CH), 7.50 (t, $J = 7.2$ Hz, 2H, 2CH), 7.37 (d, $J = 8.6$ Hz, 2H, 2CH). ^{13}C NMR (125.1 MHz, DMSO- d_6): δ 165.28, 157.45, 155.69, 153.13, 138.03, 130.79, 129.75, 129.64, 129.23, 129.19, 128.40, 127.05, 125.95, 125.82, 120.93, 117.50, 98.78. Anal. Calcd. for $C_{21}H_{13}ClN_6O_2S_2$: C, 52.44; H, 2.72; N, 17.47; found: C,

52.62; H, 3.04; N, 17.66 %. HRMS (ESI) m/z for $C_{21}H_{12}ClN_6O_2S_2^- [M - H]^-$, calculated: 479.0152, found: 479.0181. HPLC purity: 97.12 % ($t_R = 14.65$ min).

4.2.9.23. 1-(4-bromophenyl)-3-(5-((6-phenylfuro[2,3-d]pyrimidin-4-yl)thio)-1,3,4-thiadiazol-2-yl)urea (53). White solid, mp: 266–268 °C, yield: 83 %. IR (KBr) (ν_{max}/cm^{-1}): 3372 and 2995 (2NH), 1719 (C=O), 1542, 1488, 1447, 1431, 1396, 1369, 1310, 1292, 1258, 1243, 1206, 1071, 968, 836, 752, 686. 1H NMR (500.1 MHz, DMSO- d_6): δ 11.49 (s, 1H, NH), 9.44 (s, 1H, NH), 8.80 (s, 1H, CH), 7.98 (d, $J = 7.9$ Hz, 2H, 2CH), 7.66 (s, 1H, CH), 7.55 (d, $J = 7.6$ Hz, 2H, 2CH), 7.50–7.40 (m, 5H, 5CH). Anal. Calcd. for $C_{21}H_{13}BrN_6O_2S_2$: C, 48.01; H, 2.49; N, 17.47; found: C, 47.83; H, 2.77; N, 17.28 %. HRMS (ESI) m/z for $C_{21}H_{12}BrN_6O_2S_2^- [M - H]^-$, calculated: 522.9647, found: 522.9654. HPLC purity: 99.04 % ($t_R = 14.66$ min).

4.2.9.24. 1-(3-chloro-4-methylphenyl)-3-(5-((6-phenylfuro[2,3-d]pyrimidin-4-yl)thio)-1,3,4-thiadiazol-2-yl)urea (54). White solid, mp: 251–253 °C, yield: 73 %. IR (KBr) (ν_{max}/cm^{-1}): 3373 and 2988 (2NH), 1717 (C=O), 1583, 1569, 1555, 1538, 1500, 1490, 1451, 1430, 1387, 1331, 1305, 1259, 1242, 1203, 1078, 972, 831, 755, 635. 1H NMR (500.1 MHz, DMSO- d_6): δ 12.58 (s, 1H, NH), 10.45 (s, 1H, NH), 8.79 (s, 1H, CH), 7.95 (d, $J = 7.5$ Hz, 2H, 2CH), 7.88 (s, 1H, CH), 7.54 (t, $J = 7.2$ Hz, 2H, 2CH), 7.50–7.40 (m, 3H, 3CH), 7.22 (d, $J = 8.2$ Hz, 1H, CH), 2.24 (s, 3H, CH₃). ^{13}C NMR (125.1 MHz, DMSO- d_6): δ 165.33, 158.16, 155.57, 153.14, 138.99, 133.60, 132.81, 131.67, 130.76, 129.75, 129.30, 128.42, 125.98, 125.77, 118.89, 117.73, 117.43, 98.78, 19.34. Anal. Calcd. for $C_{22}H_{16}ClN_6O_2S_2$: C, 53.27; H, 3.25; N, 16.94; found: C, 53.44; H, 3.13; N, 17.12 %. HRMS (ESI) m/z for $C_{22}H_{15}ClN_6O_2S_2^- [M - H]^-$, calculated: 493.0308, found: 493.0337. HPLC purity: 96.76 % ($t_R = 14.80$ min).

4.2.9.25. 1-(3,4-dichlorophenyl)-3-(5-((6-phenylfuro[2,3-d]pyrimidin-4-yl)thio)-1,3,4-thiadiazol-2-yl)urea (55). White solid, mp: 257–259 °C, yield: 64 %. IR (KBr) (ν_{max}/cm^{-1}): 3381 and 2976 (2NH), 1708 (C=O), 1587, 1556, 1537, 1489, 1476, 1451, 1427, 1388, 1377, 1263, 1231, 1207, 1078, 977, 823, 751, 668. 1H NMR (500.1 MHz, DMSO- d_6): δ 11.59 (s, 1H, NH), 9.51 (s, 1H, NH), 8.83 (s, 1H, CH), 8.00 (d, $J = 7.5$ Hz, 2H, 2CH), 7.89 (s, 1H, CH), 7.69 (s, 1H, CH), 7.60–7.53 (m, 3H, 3CH), 7.50 (t, $J = 7.8$ Hz, 1H, CH), 7.45 (d, $J = 8.5$ Hz, 2H, 2CH). Anal. Calcd. for $C_{21}H_{12}Cl_2N_6O_2S_2$: C, 48.94; H, 2.35; N, 16.31; found: C, 49.11; H, 2.58; N, 16.56 %. HRMS (ESI) m/z for $C_{21}H_{11}Cl_2N_6O_2S_2^- [M - H]^-$, calculated: 512.9762, found: 512.9798. HPLC purity: 98.49 % ($t_R = 14.90$ min).

4.2.9.26. 1-(4-chloro-3-(trifluoromethyl)phenyl)-3-(5-((6-phenylfuro[2,3-d]pyrimidin-4-yl)thio)-1,3,4-thiadiazol-2-yl)urea (56). White solid, mp: 240–243 °C, yield: 70 %. IR (KBr) (ν_{max}/cm^{-1}): 3371 and 2984 (2NH), 1712 (C=O), 1584, 1550, 1488, 1449, 1418, 1382, 1335, 1267, 1174, 1119, 1029, 978, 835, 754, 629. 1H NMR (500.1 MHz, DMSO- d_6): δ 12.39 (s, 1H, NH), 11.25 (s, 1H, NH), 8.74 (s, 1H, CH), 8.30 (s, 1H, CH), 7.94 (d, $J = 8.2$ Hz, 1H, CH), 7.89 (d, $J = 7.7$ Hz, 2H, 2CH), 7.60–7.53 (m, 6H, 6CH). Anal. Calcd. for $C_{22}H_{12}ClF_3N_6O_2S_2$: C, 45.21; H, 2.07; N, 14.38; found: C, 45.55; H, 2.38; N, 14.51 %. HRMS (ESI) m/z for $C_{22}H_{11}ClF_3N_6O_2S_2^- [M - H]^-$, calculated: 547.0026, found: 547.0090. HPLC purity: 98.48 % ($t_R = 14.89$ min).

4.2.9.27. 1-(5-((4-methoxyphenyl)furo[2,3-d]pyrimidin-4-yl)thio)-1,3,4-thiadiazol-2-yl)-3-phenylurea (57). Yellow solid, mp: 252–254 °C, yield: 62 %. IR (KBr) (ν_{max}/cm^{-1}): 3392 and 2976 (2NH), 1711 (C=O), 1589, 1547, 1521, 1503, 1426, 1399, 1388, 1372, 1317, 1271, 1258, 1109, 1019, 974, 832, 745, 659. 1H NMR (500.1 MHz, DMSO- d_6): δ 11.31 (s, 1H, NH), 9.14 (s, 1H, NH), 8.78 (s, 1H, CH), 7.95 (d, $J = 8.1$ Hz, 2H, 2CH), 7.54–7.45 (m, 3H, 3CH), 7.40–7.30 (m, 3H, 3CH), 7.12 (d, $J = 8.1$ Hz, 2H, 2CH), 3.90 (s, 3H, OCH₃). Anal. Calcd. for $C_{22}H_{16}N_6O_3S_2$: C,

55.45; H, 3.38; N, 17.64; found: C, 55.21; H, 3.54; N, 17.85 %. HRMS (ESI) m/z for $C_{22}H_{15}N_6O_3S_2^-$ [M - H]⁻, calculated: 475.0647, found: 475.0677. HPLC purity: 97.58 % (t_R = 14.08 min).

4.2.9.28. *1-(4-methoxyphenyl)-3-(5-((6-(4-methoxyphenyl)furo[2,3-d]pyrimidin-4-yl)thio)-1,3,4-thiadiazol-2-yl)urea (58)*. Yellow solid, mp: 288–290 °C, yield: 56 %. IR (KBr) (ν_{max}/cm^{-1}): 3393 and 2924 (2NH), 1707 (C=O), 1587, 1552, 1505, 1459, 1426, 1415, 1390, 1266, 1246, 1208, 1182, 1072, 1041, 1023, 970, 821, 732, 655. ¹H NMR (500.1 MHz, DMSO- d_6): δ 11.26 (s, 1H, NH), 8.95 (s, 1H, NH), 8.88 (s, 1H, CH), 7.93 (d, J = 8.1 Hz, 2H, 2CH), 7.47 (s, 1H, CH), 7.38 (d, J = 7.9 Hz, 2H, 2CH), 7.10 (d, J = 8.1 Hz, 2H, 2CH), 6.90 (d, J = 7.9 Hz, 2H, 2CH), 3.89 (s, 3H, OCH₃), 3.72 (s, 3H, OCH₃). Anal. Calcd. for $C_{23}H_{18}N_6O_4S_2$: C, 54.53; H, 3.58; N, 16.59; found: C, 54.79; H, 3.77; N, 16.39 %. HRMS (ESI) m/z for $C_{23}H_{17}N_6O_4S_2^-$ [M - H]⁻, calculated: 505.0753, found: 505.0722. HPLC purity: 98.56 % (t_R = 14.09 min).

4.2.9.29. *1-(3-chlorophenyl)-3-(5-((6-(4-methoxyphenyl)furo[2,3-d]pyrimidin-4-yl)thio)-1,3,4-thiadiazol-2-yl)urea (59)*. Yellow solid, mp: 251–254 °C, yield: 48 %. IR (KBr) (ν_{max}/cm^{-1}): 3391 and 2922 (2NH), 1702 (C=O), 1588, 1554, 1503, 1425, 1387, 1268, 1204, 1182, 1072, 1023, 972, 841, 772, 744, 683. ¹H NMR (500.1 MHz, DMSO- d_6): δ 10.31 (s, 1H, NH), 8.75 (s, 1H, CH), 8.13 (d, J = 8.0 Hz, 2H, 2CH), 7.89 (s, 1H, CH), 7.89 (s, 1H, CH), 7.52 (d, J = 8.3 Hz, 2H, 2CH), 7.46 (s, 1H, CH), 7.30 (t, J = 8.1 Hz, 1H, CH), 7.09 (d, J = 8.0 Hz, 2H, 2CH), 7.01 (d, J = 7.8 Hz, 1H, CH), 3.89 (s, 3H, OCH₃). Anal. Calcd. for $C_{22}H_{15}ClN_6O_3S_2$: C, 51.71; H, 2.96; N, 16.45; found: C, 51.58; H, 2.84; N, 16.68 %. ESI-MS m/z : 510.22 [M]⁺. HRMS (ESI) m/z for $C_{22}H_{14}ClN_6O_3S_2^-$ [M - H]⁻, calculated: 509.0257, found: 509.0283. HPLC purity: 98.84 % (t_R = 14.63 min).

4.2.9.30. *1-(4-chlorophenyl)-3-(5-((6-(4-methoxyphenyl)furo[2,3-d]pyrimidin-4-yl)thio)-1,3,4-thiadiazol-2-yl)urea (60)*. Yellow solid, mp: 291–293 °C, yield: 59 %. IR (KBr) (ν_{max}/cm^{-1}): 3388 and 2923 (2NH), 1710 (C=O), 1544, 1505, 1487, 1425, 1385, 1307, 1268, 1181, 1014, 971, 835, 744, 699, 615. ¹H NMR (500.1 MHz, DMSO- d_6): δ 11.40 (s, 1H, NH), 9.28 (s, 1H, NH), 8.77 (s, 1H, CH), 7.93 (d, J = 8.0 Hz, 2H, 2CH), 7.53 (d, J = 8.3 Hz, 2H, 2CH), 7.48 (s, 1H, CH), 7.38 (d, J = 8.3 Hz, 2H, 2CH), 7.10 (d, J = 8.0 Hz, 2H, 2CH), 3.90 (s, 3H, OCH₃). Anal. Calcd. for $C_{22}H_{15}ClN_6O_3S_2$: C, 51.71; H, 2.96; N, 16.45; found: C, 51.98; H, 3.12; N, 16.73 %. HRMS (ESI) m/z for $C_{22}H_{14}ClN_6O_3S_2^-$ [M - H]⁻, calculated: 509.0257, found: 509.0233. HPLC purity: 96.81 % (t_R = 14.62 min).

4.2.9.31. *1-(4-chloro-3-(trifluoromethyl)phenyl)-3-(5-((6-(4-methoxyphenyl)furo[2,3-d]pyrimidin-4-yl)thio)-1,3,4-thiadiazol-2-yl)urea (61)*. Yellow solid, mp: 265–267 °C, yield: 53 %. IR (KBr) (ν_{max}/cm^{-1}): 3384 and 2920 (2NH), 1703 (C=O), 1590, 1539, 1428, 1385, 1315, 1268, 1249, 1221, 1178, 1079, 1032, 974, 839, 722, 683. ¹H NMR (500.1 MHz, DMSO- d_6): δ 10.11 (s, 1H, NH), 8.84 (s, 1H, CH), 8.25 (s, 1H, CH), 7.98 (d, J = 8.0 Hz, 2H, 2CH), 7.84 (d, J = 8.9 Hz, 1H, CH), 7.58 (d, J = 8.9 Hz, 1H, CH), 7.44 (s, 1H, CH), 7.09 (d, J = 8.0 Hz, 2H, 2CH), 3.90 (s, 3H, OCH₃). Anal. Calcd. for $C_{23}H_{14}ClF_3N_6O_3S_2$: C, 47.71; H, 2.44; N, 14.52; found: C, 47.98; H, 2.63; N, 14.82 %. HRMS (ESI) m/z for $C_{23}H_{13}ClF_3N_6O_3S_2^-$ [M - H]⁻, calculated: 577.0131, found: 577.0154. HPLC purity: 97.05 % (t_R = 15.33 min).

4.2.10. HPLC method for the analysis of isolated compounds

The HPLC analysis was performed on a Waters Alliance HPLC system equipped with a Waters 2998 photodiode array detector. Separation was achieved using 25.0 cm × 4.6 mm; 5 μ m packing C18 (L1 USP) column for LC. The mobile phase A was ammonium acetate buffer (10 mM, pH 2.5), and the mobile phase B was acetonitrile. A gradient elution was employed as follows: 0–14 min, 20 % B; 15–35 min, 40 % B; 36–45 min, 20 % B. The flow rate was set at 1.0 mL/min. The column temperature

was maintained at 25 °C, and the injection volume was 10 μ L. Detection was carried out at 260 nm. Samples were prepared by diluting the isolated compounds in DMSO: Acetonitrile (10 : 90 %V/V) to a final concentration of 1 mg/mL and filtering through a 0.45 μ m PTFE syringe filter before injection.

4.2.11. Kinase-inhibitory assays

Activities of novel compounds against recombinant FLT3-ITD and FLT3-ITD-F691L kinases were analyzed as described previously [46].

Protein kinase selectivity of compound **49** was evaluated at a single concentration (1 μ M) by screening against 50 enzymes (Express Screen Panel) at MRC Protein Phosphorylation and Ubiquitylation Unit, University of Dundee.

4.2.12. Cell culture and proliferation assay

Human cell lines were obtained from the German Collection of Microorganisms and Cell Cultures (MOLM-13, EOL-1, Kasumi-1), the Cell Lines Service (MV4-11), and the European Collection of Authenticated Cell Cultures (K562, HL60, HEK293), and were cultivated according to the providers' instructions. Murine Ba/F3 cells stably transfected with FLT3-ITD and FLT3-ITD-F691L were kindly provided by Prof. R. Zeiser (University of Freiburg, Germany). Briefly, MV4-11, MOLM-13, EOL-1, Kasumi-1, Ba/F3 FLT3-ITD and Ba/F3 FLT3-ITD-F691L were maintained in RPMI-1640 medium, HL60 in IMDM, K562 in DMEM, and HEK293 in EMEM medium. Murine parental Ba/F3 cell line was maintained in RPMI-1640 medium with murine IL-3 (2 ng/mL). The cell culture medium was supplemented with 10 % fetal bovine serum, penicillin (100 U/mL), and streptomycin (100 μ g/mL) and cells were cultivated at 37 °C in 5 % CO₂.

For antiproliferative assays, cells seeded into 96-well plates in appropriate densities were treated with test compounds. After the incubation period, resazurin (Merck) solution was added for 4 h. Fluorescence of resorufin corresponding to live cells was measured at 544 nm/590 nm (excitation/emission) using a Fluoroskan Ascent microplate reader (Labsystems).

4.2.13. NanoBRET target engagement assay

The NanoBRET Target Engagement Intracellular Kinase Assay K-10 (N2640, Promega) was performed in human kidney embryonal HEK293 cells using polyethylenimine (PEI) transfection. Transfection mixture was prepared with 5 μ g of plasmid encoding FLT3-NanoLuc® Fusion Vector (NV1391, Promega) and 10 μ g of PEI solution (Merck) diluted in 1 mL of EMEM media without phenol red. After 15 min, transfection complex was added to HEK293 cells in suspension and the cells were seeded in 96-well μ Clear®-bottom white plate (Greiner Bio-One) at the density of 30 000 cells per well and incubated in a humidified CO₂ incubator at 37 °C. The next day, NanoBRET™ Tracer K-10 at 100 nM concentration was added to plate and after 15 min, also tested compounds were added in different concentrations in duplicate, and plates were incubated for additional 2 h before assaying for BRET measurements. Separately, FLT3-NanoLuc® kinase expression was confirmed by Western blot using anti-NanoLuc antibody (N7000, Promega). NanoBRET™ Nano-Glo® Substrate and Extracellular NanoLuc® Inhibitor (N2640, Promega) were diluted according to the manufacturer's instructions and added to plate, and luminescence signal (Chroma-Glo application, 460–545 nm emission for donor and 610–700 nm for acceptor, respectively) was read using a Spark reader (Tecan). BRET ratio was generated by dividing the acceptor emission values by the donor emission values for each sample, and converted to mBRET by multiplying each raw value by 1000. The engagement data were normalized to no drug (=100 %) and no tracer (=0 %) and fit using Origin software (version 6.0).

4.2.14. Cell cycle analysis

Leukemia cells were seeded and, after a preincubation period, treated with tested compounds for 24 h. After staining with propidium

iodide, DNA content was analyzed by flow cytometry using a 488 nm laser (BD FACSVerser with BD FACSuite software, version 1.0.6). Cell cycle distribution was analyzed using ModFit LT (Verity Software House).

4.2.15. Immunoblotting

Cell lysates were separated on SDS-polyacrylamide gels and electroblotted onto nitrocellulose membranes. After blocking, proteins were incubated first with specific primary antibodies and subsequently with peroxidase-conjugated secondary antibodies. Peroxidase activity was detected using SuperSignal West Pico reagents (Thermo Fisher Scientific) and the LAS-4000 CCD camera system (Fujifilm). The following specific antibodies were purchased from Cell Signaling Technology: anti-FLT3 (8F2), anti-phospho-FLT3 Y589/591 (30D4), anti-STAT5 (D2O6Y), anti-phospho-STAT5 Y694, anti-ERK1/2, anti-phospho-ERK1/2 (T202/Y204). Anti-PCNA (clone PC-10) was generously gifted by Dr. Bořivoj Vojtěšek (Masaryk Memorial Cancer Institute, Brno).

4.2.16. Molecular docking studies

Molecular docking was performed into the co-crystal of inactive FLT3 with quizartinib (PDB: 4XUF) [40]. The 3D structure of **49** and several conformations with the lowest energy were prepared using molecular mechanics with Avogadro 1.90.0. Ligand was adjusted and polar hydrogens were added to ligand and protein with the AutoDock Tools. The rigid docking was performed in AutoDock Vina 1.05938 [47]. Interactions between **49** or quizartinib and FLT3 were determined using Biowia Discovery Studio 2021, ver. 21.1.0.20298 (Dassault Systemes, Vélizy-Villacoublay, France) and the figures were generated using Pymol ver. 2.0.4 (Schrödinger, LLC, New York, NY, USA).

CRediT authorship contribution statement

Mahfam Moradi: Writing – original draft, Investigation. **Alireza Mousavi:** Writing – original draft, Investigation. **Eva Řezníčková:** Writing – review & editing, Writing – original draft, Investigation, Conceptualization. **Fariba Peytam:** Writing – review & editing, Writing – original draft, Conceptualization. **Miroslav Perina:** Investigation. **Veronika Vojáčková:** Investigation. **Loghman Firoozpour:** Investigation. **Radek Jorda:** Investigation, Formal analysis. **Jiří Grúz:** Writing – original draft, Investigation, Data curation. **Zahra Emamgholipour:** Investigation. **Sayed Esmaeil Sadat-Ebrahimi:** Investigation. **Vladimír Kryštof:** Writing – review & editing, Writing – original draft, Supervision, Funding acquisition, Conceptualization. **Alireza Foroumadi:** Writing – review & editing, Writing – original draft, Supervision, Funding acquisition, Conceptualization.

Declaration of competing interest

The authors declare that they have no known competing financial interests or personal relationships that could have appeared to influence the work reported in this paper.

Acknowledgements

The authors wish to thank Tomáš Pospíšil for consulting on NMR. This work was financially supported by Tehran University of Medical Sciences (grants 1403-2-104-66006 and 1402-3-263-68726), the European Union - Next Generation EU (The project National Institute for Cancer Research, Programme EXCELES, ID No. LX22NPO5102), Czech Science Foundation (23-05462S) and Palacký University Olomouc (IGA_PrF_2024_005).

Appendix A. Supplementary data

Supplementary data to this article can be found online at <https://doi.org/10.1016/j.ejmech.2024.116962>.

Data availability

Data will be made available on request.

References

- [1] H. Döhner, D.J. Weisdorf, C.D. Bloomfield, Acute myeloid leukemia, *N. Engl. J. Med.* 373 (12) (2015) 1136–1152.
- [2] R.M. Shallis, et al., Epidemiology of acute myeloid leukemia: recent progress and enduring challenges, *Blood Rev.* 36 (2019) 70–87.
- [3] H. Liu, Emerging agents and regimens for AML, *J. Hematol. Oncol.* 14 (1) (2021) 49.
- [4] T. Oellerich, et al., FLT3-ITD and TLR9 use Bruton tyrosine kinase to activate distinct transcriptional programs mediating AML cell survival and proliferation, *Blood* 125 (12) (2015) 1936–1947.
- [5] Y. Zhong, et al., Small-molecule fms-like tyrosine kinase 3 inhibitors: an attractive and efficient method for the treatment of acute myeloid leukemia, *J. Med. Chem.* 63 (21) (2020) 12403–12428.
- [6] H. Drexler, Expression of FLT3 receptor and response to FLT3 ligand by leukemic cells, *Leukemia* 10 (4) (1996) 588–599.
- [7] S. Takahashi, Downstream molecular pathways of FLT3 in the pathogenesis of acute myeloid leukemia: biology and therapeutic implications, *J. Hematol. Oncol.* 4 (2011) 1–10.
- [8] J.C. Zhao, et al., A review of FLT3 inhibitors in acute myeloid leukemia, *Blood Rev.* 52 (2022) 100905.
- [9] F.A. Lagunas-Rangel, V. Chávez-Valencia, FLT3-ITD and its current role in acute myeloid leukaemia, *Med. Oncol.* 34 (2017) 1–13.
- [10] S. Li, et al., FLT3-TKD in the prognosis of patients with acute myeloid leukemia: a meta-analysis, *Front. Oncol.* 13 (2023) 1086846.
- [11] A. Sudhindra, C.C. Smith, FLT3 inhibitors in AML: are we there yet? *Curr. Hematol. Malig. Rep.* 9 (2014) 174–185.
- [12] A. Antar, et al., Inhibition of FLT3 in AML: a focus on sorafenib, *Bone Marrow Transplant.* 52 (3) (2017) 344–351.
- [13] W. Fiedler, et al., Sunitinib and intensive chemotherapy in patients with acute myeloid leukemia and activating FLT3 mutations: results of the AMLSG 10-07 Study (ClinicalTrials.gov No. NCT00783653), *Blood* 120 (21) (2012) 1483.
- [14] M.M. Schittenhelm, et al., The FLT3 inhibitor tandutinib (formerly MLN518) has sequence-independent synergistic effects with cytarabine and daunorubicin, *Cell Cycle* 8 (16) (2009) 2621–2630.
- [15] M. Levis, Midostaurin approved for FLT3-mutated AML, *Blood* 129 (26) (2017) 3403–3406.
- [16] A.T. Fathi, M. Levis, Lestaurtinib: a multi-targeted FLT3 inhibitor, *Expert Rev. Hematol.* 2 (1) (2009) 17–26.
- [17] E. Weisberg, et al., Antileukemic effects of novel first-and second-generation FLT3 inhibitors: structure-affinity comparison, *Genes Cancer* 1 (10) (2010) 1021–1032.
- [18] J. Zhao, Y. Song, D. Liu, Gilteritinib: a novel FLT3 inhibitor for acute myeloid leukemia, *Biomark. Res.* 7 (2019) 19.
- [19] A. Galanis, et al., Crenolanib is a potent inhibitor of FLT3 with activity against resistance-conferring point mutants, *Blood* 123 (1) (2014) 94–100, <https://doi.org/10.1182/blood-2013-10-529313>.
- [20] N. Daver, et al., Tuspentinib myeloid kinase inhibitor safety and efficacy as monotherapy and combined with venetoclax in phase 1/2 trial of patients with relapsed or refractory (R/R) acute myeloid leukemia (AML), *Blood* 142 (2023) 162.
- [21] S.A. Wander, M.J. Levis, A.T. Fathi, The evolving role of FLT3 inhibitors in acute myeloid leukemia: quizartinib and beyond, *Ther. Adv. Hematol.* 5 (3) (2014) 65–77.
- [22] M.T. Gebru, H.-G. Wang, Therapeutic targeting of FLT3 and associated drug resistance in acute myeloid leukemia, *J. Hematol. Oncol.* 13 (2020) 1–13.
- [23] S.S. Lam, A.Y. Leung, Overcoming resistance to FLT3 inhibitors in the treatment of FLT3-mutated AML, *Int. J. Mol. Sci.* 21 (4) (2020) 1537.
- [24] L.M. Jones, et al., Targeting AML-associated FLT3 mutations with a type I kinase inhibitor, *J. Clin. Investig.* 130 (4) (2020) 2017–2023.
- [25] M.M. Aly, et al., A systematic review and meta-analysis comparing type I and II FLT3 inhibitors in relapsed/refractory acute myeloid leukemia and high-risk myelodysplastic syndrome, *Blood* 138 (2021) 1249.
- [26] M. Beyer, et al., Identification of a highly efficient dual type I/II FMS-like tyrosine kinase inhibitor that disrupts the growth of leukemic cells, *Cell Chem. Biol.* 29 (3) (2022) 398–411, <https://doi.org/10.1016/j.chembiol.2021.10.011>.
- [27] A.S. Alotaibi, et al., Patterns of resistance differ in patients with acute myeloid leukemia treated with type I versus type II FLT3 inhibitors, *Blood Cancer Discov.* 2 (2) (2021) 125–134.
- [28] S. Meshinchi, F.R. Appelbaum, Structural and functional alterations of FLT3 in acute myeloid leukemia, *Clin. Cancer Res.* 15 (13) (2009) 4263–4269.
- [29] M.S. Coumar, et al., Identification, SAR studies, and X-ray Co-crystallographic analysis of a novel furanopyrimidine Aurora kinase A inhibitor, *ChemMedChem* 5 (2) (2010) 255–267.
- [30] M.-C. Li, et al., Development of furanopyrimidine-based orally active third-generation EGFR inhibitors for the treatment of non-small cell lung cancer, *J. Med. Chem.* 66 (4) (2023) 2566–2588.
- [31] A. Zhao, et al., Discovery of novel c-Met kinase inhibitors bearing a thieno[2,3-d]pyrimidine or furo[2,3-d]pyrimidine scaffold, *Bioorg. Med. Chem.* 19 (13) (2011) 3906–3918.

- [32] M.M. Abd El-Mageed, et al., Design and synthesis of novel furan, furo[2,3-d] pyrimidine and furo[3,2-e][1,2,4]triazolo[1,5-c]pyrimidine derivatives as potential VEGFR-2 inhibitors, *Bioorg. Chem.* 116 (2021) 105336.
- [33] Y. Chang Hsu, et al., Facile identification of dual FLT3–Aurora A inhibitors: a computer-guided drug design approach, *ChemMedChem* 9 (5) (2014) 953–961.
- [34] W.-W. Li, et al., Discovery of the novel potent and selective FLT3 inhibitor 1-(5-[7-(3-morpholinopropoxy)quinazolin-4-ylthio]-[1,3,4] thiadiazol-2-yl)-3-p-tolylurea and its anti-acute myeloid leukemia (AML) activities in vitro and in vivo, *J. Med. Chem.* 55 (8) (2012) 3852–3866.
- [35] A. Faraji, et al., Design, synthesis and evaluation of novel thienopyrimidine-based agents bearing diaryl urea functionality as potential inhibitors of angiogenesis, *Eur. J. Med. Chem.* 209 (2021) 112942.
- [36] R. Motahari, et al., Design, synthesis and evaluation of novel tetrahydropyridothienopyrimidin-ureas as cytotoxic and anti-angiogenic agents, *Sci. Rep.* 12 (1) (2022) 9683.
- [37] M. Shafiei, et al., Design, synthesis, and in vitro and in vivo evaluation of novel fluconazole-based compounds with promising antifungal activities, *ACS Omega* 6 (38) (2021) 24981–25001.
- [38] D.D. Erol, et al., Synthesis and biological activities of some 3,6-disubstituted Thiazolo[3,2-b][1,2,4]triazoles, *J. Pharm. Sci.* 84 (4) (1995) 462–465.
- [39] M.M. Ramiz, A.A. Abdel-Rahman, Antimicrobial activity of newly synthesized 2,5-disubstituted 1,3,4-thiadiazole derivatives, *Bull. Kor. Chem. Soc.* 32 (12) (2011) 4227–4232.
- [40] J.A. Zorn, et al., Crystal structure of the FLT3 kinase domain bound to the inhibitor Quizartinib (AC220), *PLoS One* 10 (4) (2015) e0121177.
- [41] S.-S. Ge, S.-B. Liu, S.-L. Xue, Developments and challenges of FLT3 inhibitors in acute myeloid leukemia, *Front. Oncol.* 12 (2022) 996438.
- [42] R. Assi, F. Ravandi, FLT3 inhibitors in acute myeloid leukemia: choosing the best when the optimal does not exist, *Am. J. Hematol.* 93 (4) (2018) 553–563.
- [43] A.A. Warkentin, et al., Overcoming myelosuppression due to synthetic lethal toxicity for FLT3-targeted acute myeloid leukemia therapy, *Elife* 3 (2014) e03445.
- [44] C. Albers, et al., The secondary FLT3-ITD F691L mutation induces resistance to AC220 in FLT3-ITD+ AML but retains in vitro sensitivity to PKC412 and Sunitinib, *Leukemia* 27 (6) (2013) 1416–1418.
- [45] C.C. Smith, et al., Activity of ponatinib against clinically-relevant AC220-resistant kinase domain mutants of FLT3-ITD, *Blood* 121 (16) (2013) 3165–3171.
- [46] P. Brehova, et al., Inhibition of FLT3-ITD kinase in acute myeloid leukemia by new imidazo[1,2-b]pyridazine derivatives identified by scaffold hopping, *J. Med. Chem.* 66 (16) (2023) 11133–11157.
- [47] O. Trott, A.J. Olson, AutoDock Vina: improving the speed and accuracy of docking with a new scoring function, efficient optimization, and multithreading, *J. Comput. Chem.* 31 (2) (2010) 455–461.